



Collecting Antiprotons in the Fermilab Booster and Very High  
Energy Proton-Antiproton Interactions

D. Cline, P. McIntyre, F. Mills and C. Rubbia\*

Fermilab  
P.O. Box 500  
Batavia, Illinois 60510

Department of Physics  
Harvard University  
Cambridge, Massachusetts 02138

Department of Physics  
University of Wisconsin  
Madison, Wisconsin 53706

ABSTRACT

We describe a technique for producing an intense beam of antiprotons to be used for very high energy  $\bar{p}$ -p colliding beams. The Fermilab Booster is to be used as a collector for antiprotons produced on an external target. The antiprotons are decelerated and transferred to a 200 MeV storage ring (Freezer Ring) and then collapsed in phase space by electron cooling. Repetitive accumulation over  $10^4$ - $10^5$  Booster pulses, acceleration to 8 GeV and injection into the main ring lead to the possibility of  $\bar{p}p$  collisions at several hundred GeV with luminosity in excess of  $10^{29} \text{ cm}^{-2} \text{ sec}^{-1}$ .

\*Presently at CERN, Geneva, Switzerland.



## Contents

I.	Introduction	1
II.	Main Physics Motivations	5
III.	Antiproton Production and Deceleration	10
	1. Introduction	10
	2. Gymnastics on Proton Beam, Extraction and Targeting	11
	3. Bunch Synchronization	12
	4. Production and Collection of Antiprotons	14
IV.	Antiproton Storage and Cooling	17
	1. Design Criteria	17
	2. Magnetic Structure	18
	3. Long Straight Sections for Electron Cooling	20
	4. Vacuum System	20
	5. Electron Cooling	22
	6. Electron Beam and Electron Gun	26
	7. Stacking in the Freezer	27
V.	$\bar{P}P$ Collisions in the Main Ring	28
VI.	$\bar{P}$ Beam Regeneration	30
	Acknowledgements	32
	Appendices	35
I.	Initial Experimental Test of Electron Cooling - Racetrack Ring Set-up on the Surface	35
II.	Theory of Electron Confinement in a Magnetic Field	36
III.	Freezer Ring as an Accumulator and Proton Cooler to Increase Luminosity	47



## I. INTRODUCTION

It is an old dream of particle physicists to construct a proton-antiproton colliding beam machine. High energy accelerator beams produce copious numbers of antiprotons. Recently we<sup>1</sup> have pointed out that the existing high energy rings at CERN and Fermilab can be transformed into  $\bar{p}p$  storage rings of about 800 GeV in the center of mass. Furthermore the forthcoming Energy Doubler/Saver at Fermilab could give access to the fantastic energy of 2 TeV in the center of mass and would be quite suitable for a high performance storage ring.<sup>2</sup> In order to transform existing machines into  $\bar{p}p$  colliding beams a method must be devised to collect and cool the antiproton phase space followed by reinjection of the  $\bar{p}$  beam into the storage ring. Several methods have been devised to carry out this repetitive accumulation and cooling.<sup>3,4,5</sup>

A fundamental progress in this direction has been accomplished by the Novosibirsk group, which has recently demonstrated the possibility of damping betatron motions and momentum spread of 80 MeV protons with the help of collinear electrons traveling at the same speed<sup>3</sup> (electron cooling). In these beautiful experiments the proton beam size collapses to sub millimetric dimensions and  $\Delta p/p \sim 10^{-5}$  in about 80 milliseconds.<sup>6</sup>

In order to adapt this technique to antiproton cooling, one faces the problem that phase space compression with electrons works efficiently only at non-relativistic energies ( $\tau \sim \beta^4 \gamma^5$ ), while the greatest majority of  $\bar{p}$ 's are produced fast in the laboratory system, i.e.  $\langle \gamma_{\bar{p}} \rangle \sim \sqrt{E_p/2m}$ . For instance for  $E_p = 100$  GeV  $\langle \gamma_{\bar{p}} \rangle \approx 7$  and the cooling time will then increase

by the factor  $2^4 \cdot 7^5 = 260,000!!$  Furthermore the technological problems associated with an electron cooler operating at  $\gamma = 7$  are formidable<sup>6</sup>, (e.g. the electron accelerating voltage must be 3.5 million volts) and they have not been satisfactorily solved to date.

It has occurred to us that one could bridge the gap between optimum production and cooling energies for antiprotons by introducing an additional stage of deceleration between the production of  $\bar{p}$ 's and the subsequent electron cooling<sup>7</sup>. We elaborate a realistic scheme making use of the rapid cycles of the Fermilab booster to decelerate  $\bar{p}$ 's to 200 MeV where we could perform Budker-type cooling and stacking in a modest ring (Freezer) housed in the same tunnel.

We believe this scheme has several attractive features among which are the availability of the major components, their inherent reliability, and the modest nature of the required 200 MeV storage ring. It could be carried out at modest cost and with very little need for new technological innovations. Thus within a few years the Fermilab accelerator can be transformed into a high energy  $\bar{p}p$  storage ring device.

The scheme consists of three separate phases:

i. Antiproton production, deceleration and accumulation.

Secondary particles at about 6.5 GeV/c are produced by 100 GeV/c protons from the main ring impinging on a small tungsten target. Particles are injected into the booster ring and decelerated to 200 MeV. Only  $\bar{p}$ 's survive at the end of the process.

The beam is transferred to the storage ring where it is cooled and added to the stack of previous accumulations.

One expects to accumulate  $4 \times 10^7$   $\bar{p}$ /pulse leading to  $\sim 10^{11}$  particles in  $2 \times 10^3$  pulses (3 hours).

ii. Injection of p and  $\bar{p}$  in the main ring, and experimentation in  $p\bar{p}$  collisions. The  $\bar{p}$  beam is transferred from the Freezer to the Booster, accelerated to 8 GeV, and reverse injected in the main ring (MR). A standard proton Booster pulse is then injected in the main ring, with appropriate phasing in order to give collisions at the desired point of the main ring. There are then 84 proton and 84 antiproton bunches counter-rotating. With  $10^{11}$   $\bar{p}$ 's and  $4 \times 10^{12}$  p's with standard emittances, we expect a luminosity of  $\sim 10^{29}$   $\text{sec}^{-1}\text{cm}^{-2}$  in the low-beta section designed by T. Collins. The scheme is shown in Fig. 1.

iii. Antiproton beam regeneration. After some time, beam-gas scattering, R.F. noise and higher order resonances could lead to an appreciable blow-up of the beams with consequent loss of luminosity. In order to restore beam quality, we propose to dump the proton beam, decelerate  $\bar{p}$ 's first in the MR to 8 GeV then in the Booster to 200 MeV, then cool again in the Freezer. The cooling process should take only seconds. After this,  $\bar{p}$ 's are accelerated again by the Booster, injected in the MR with a new companion proton beam and accelerated to high energies.

The main open question is how well electron cooling works. The recent results of Budker's group at Novosibirsk have shown that it is possible to cool a modest proton beam of 50-80 MeV in less than 100 msec. This impressive result allows one to attempt extrapolations to our conditions. However it is clearly imperative to perform additional experimentation at Fermilab on cooling techniques (see Appendix I, III).

## II. MAIN PHYSICS MOTIVATIONS

The past ten years have seen remarkable progress in the understanding of elementary particles. First there is the experimental discovery of  $\Delta S = 0$  weak neutral currents,<sup>8</sup> which when contrasted with the previous limits on  $\Delta S = 1$  neutral current decay processes<sup>9</sup> leads to the suggestion of additional hadronic quantum numbers in nature.<sup>10</sup> Evidence now exists for new hadronic quantum numbers that are manifested either directly<sup>11,12</sup> or indirectly.<sup>13</sup> The experimental discoveries are complemented by the theoretical progress of unified gauge theories.<sup>14</sup> These developments lead to the expectation that very massive intermediate vector bosons ( $50 - 100 \text{ GeV}/c^2$ ) may exist in nature.<sup>14</sup> The search for these massive bosons and other new phenomena require three separate elements to be successful: a reliable physical mechanism for production, very high center of mass energies, and an unambiguous experimental signature to observe them. In addition to the high center-of-mass energy available in  $\bar{p}$ -p collisions, several considerations suggest that they may present a much better opportunity of discovering new phenomena than p-p collisions.<sup>15</sup>

First we consider production process. There is now very strong support for the notion of pointlike constituents in the hadron obtained from lepton-hadron scattering and very high energy neutrino experiments. The experimental detection of weak interaction processes in hadronic collisions almost certainly involve quark-antiquark (or proton-antiproton) annihilation.

lation processes very much like  $e^+ e^-$  collisions. (For example, the processes  $u + \bar{u} \rightarrow \mu^+ + \bar{\mu}$  or  $u + \bar{d} \rightarrow \mu + \nu$ .) There are clearly more antiquarks in an antiproton, than in a proton, and furthermore the antiquarks in an antiproton, being valence quarks, carry a much larger fraction of the total energy than do the (sea) antiquarks in a proton. The exact size of these effects at high energy are uncertain, but qualitatively cross sections probably differ by a factor up to 10 - 100 in favor of the  $\bar{p}p$  system.

The  $\bar{p}p$  system is an eigenstate of charge conjugation (C) invariance whereas the  $pp$  system is not. Thus there are many simple experimental tests of C violation in the  $\bar{p}p$  system. The observation of C violation may be an important technique to observe the effects of weak interactions in very high energy collisions. In the case of the  $pp$  system the "equivalent" way to observe weak interaction effects is through parity violation. This very likely involves polarization measurements which are considerably more difficult than tests of C violation. Thus proton-antiproton collisions at the highest energy offer distinct advantages in the search for new phenomena in nature, especially those associated with the weak interaction.

We now turn to the specific case of the production and detection of the weakly interacting intermediate vector bosons. Present neutrino data indicate a mass limit of  $>20$  GeV for the charged intermediate vector boson.<sup>16</sup> The center-of-mass energy available in a proton-antiproton storage ring is .4-2.0 TeV, sufficient to produce very large mass intermediate vector

bosons. In the Weinberg-Salam model the  $W^0$  the  $W^\pm$  1,14,16 masses are now estimated to be  $80 \pm 6$  GeV and  $64 \pm 11$  GeV, respectively. This mass is outside the reach of the presently planned new generation of  $e^+e^-$  storage rings.

The derivation of the  $W^0$  cross section exposes the basic simplicity of the assumptions for the case of  $\bar{p}p$  collisions.<sup>1,15</sup> By analogy the  $\bar{q}q$  annihilation behaves like  $e^+e^-$  scattering. In the  $e^+e^-$  case a sharp resonance peak would be expected in the cross section for the process

$$\begin{aligned}
 e^+ + e^- &\rightarrow W^0 \rightarrow e^+ + e^- \\
 &\rightarrow \mu^+ + \mu^- \\
 &\rightarrow u + \bar{u} \quad (\text{hadron}) + (\text{antihadrons}) \\
 &\quad d + \bar{d} \quad (\text{jet}) \quad \quad (\text{jet})
 \end{aligned}$$

In order to estimate the cross section for  $\bar{p}p$  collisions the structure functions of partons must be known. Neutrino and charged lepton scattering experiments provide the necessary structure functions and have set limits ( $>20$  GeV) on any non-locality in the parton form factor.<sup>17</sup> The main difference with respect to  $e^+e^-$  is that now the kinematics is largely smeared out by the internal motion of the  $q$ 's and  $\bar{q}$ 's. The average center of mass energy squared of the  $q\bar{q}$  collision is roughly

$$\langle S_{q\bar{q}} \rangle \sim S \langle x_q \rangle_p \langle x_{\bar{q}} \rangle_{\bar{p}}$$

where  $S$  is the center of mass energy squared of the  $\bar{p}p$  system and  $\langle x_q \rangle_p = \langle x_{\bar{q}} \rangle_{\bar{p}}$  we find  $\langle S_{q\bar{q}} \rangle \sim 0.04 S$ . For  $M = 100 \text{ GeV}/c^2$

this suggests  $S > 2 \times 10^5 \text{ GeV}^2$  or  $\sqrt{S} \geq 450 \text{ GeV}$ . In the case of pp scattering the  $\langle x_{\bar{q}p} \rangle$  is expected to be much less and the  $x$  distribution probably falls very rapidly.

Detailed estimates have been given by several authors<sup>1,15</sup> and give

$$\sigma(\bar{p}p \rightarrow W^0 + \text{hadrons} \rightarrow e^+ + e^- + \text{hadrons}) \approx 10^{-32} \text{ cm}^2$$

More optimistic cross section estimates also exist in the literature.<sup>18</sup>

The cross section estimated above leads to 3.6 events/hour given a luminosity of  $10^{29} \text{ cm}^{-2} \text{ sec}^{-1}$  and 100% detection efficiency. The  $\mu^+\mu^-$  is expected to be very small compared to the  $W^0$  signal. Furthermore if the  $W^0$  decay into hadronic states is detected the corresponding event rate will increase. We note that since the  $q$  and  $\bar{q}$  have comparable  $x$  distributions in  $\bar{p}p$  collisions, a large fraction of the  $W$ 's produced will have low  $x_W$  and hence decay symmetrically in the lab. In  $pp$  collisions, the widely different  $q$  and  $\bar{q}$   $x$  distribution can produce sizeable  $x_W$ . Finally the charged vector bosons may well have lower mass and thus larger cross sections, with a somewhat weaker experimental signature.

Another challenging possibility is a search for fractionally charged quarks. Overwhelming evidence favors the existence of light, fractionally charged constituents inside the hadrons. Absence of direct production of free quarks suggests the existence of confinement mechanisms (bag). It is not known, but it appears likely that at very high energies the "bag" could be broken, thus liberating the elementary constituents. A search for quarks in very high energy hadron-hadron collisions is mandatory.

Finally there is one additional possibility for interesting and unique physics with the low energy antiproton storage ring itself. It appears that the present universe has a net positive baryon number for unknown reasons. A simple, but seemingly unlikely possibility is that the antiproton is unstable and has a lifetime much shorter than  $10^{10}$  years. The present limit on the antiproton lifetime is likely no better than milliseconds. Using a small antiproton storage ring with  $10^{10} - 10^{12}$  antiprotons stored for periods of days it appears possible to detect an unstable antiproton if the lifetime is less than  $\sim 10^7$  years. This must be considered a long shot but we know of no other way to discover antiproton disintegration.

The observation of an unstable antiproton, coupled with the observed stability of the proton ( $>10^{29}$  years); would violate the PCT theorem.

### III. ANTIPROTON PRODUCTION AND DECELERATION

#### III-1. Introduction

In this phase, the Booster is alternately accelerating 12 proton pulses and decelerating 12 antiproton pulses (see Fig. 2). The settings of the magnetic cycles are unchanged. However, the rf is turned on alternately on the rising and falling sides of the magnet ramp and the phase sequence among cavities is inverted. Since the  $p$  and  $\bar{p}$  currents are vastly different ( $4 \times 10^{12} p$  vs  $3 \times 10^7 \bar{p}$ ) two separate beam control systems will be necessary. In order to ease the extraction of the 100 GeV primary protons, 12 Booster pulses are injected in the Main Ring, leaving a time gap between pulses to allow for the rise and fall times of the kicker magnet. We propose to eject the beam from the medium straight section F17 and to transport it along the newly-planned line from there to the Booster (Fig. 1 and Fig. 3). Targeting and the beam dump occur along this line, and  $\bar{p}$ 's can be reverse injected in the Booster through the new 8-GeV proton extraction channel. We have taken the "good field" Booster ring acceptances<sup>19</sup> at 200 MeV and adiabatic extrapolation to other energies. We understand that these goals have not been reached as yet and that more work is necessary.<sup>20</sup>

III-2. Gymnastics on Proton Beam, Ejection and Targeting.

The largest possible beam current is accelerated to 100 GeV/c, then the main ring is flat-topped with rf at maximum voltage. With  $V_{rf} = 3.4 \times 10^6$  Volt,  $h = 1113$ ,  $f = 53.4$  kHz and  $\eta = 3.3 \times 10^{-3}$  we calculate

$$v_s = [\hbar \eta \text{ eV}/2\pi \text{ E}]^{1/2} = 3.65 \times 10^{-3}$$

The bunching factor B (bunch length/bunch separation) is then

$$B = \left(\frac{h}{2\pi}\right) (8f\eta/p v_s)^{1/2} A_b^{1/2} = 0.27 A_b^{1/2}$$

where  $A_b$  is the invariant bunch area, expressed in eV - sec. Taking  $A_b = 0.1$  eV sec, which is about four times the injection area in the booster, we get

$$B = 0.085$$

$$\frac{\Delta p}{p} / \text{full} = \frac{1}{\beta} \left[ 8A_b f v_s / p\eta \right]^{1/2} = 1.67 \times 10^{-3}$$

We eject 84 bunches of the main ring at a time and focus the beam on a very small tungsten target. The extraction of 100-GeV protons is shown in Fig. 3. At position E48 in the Main Ring, there is a missing magnet position giving a straight section of 7m available length. A pulsed magnetic kicker  $S_1$  at that position produces a horizontal bump of 3cm at the medium straight section F17 ( $\Delta v = 0.81$ ). There exists there an available length of 14m. Two Lambertson septa  $S_2$  will deflect the beam vertically by 25 mrad, producing a deflection of 18 cm at the face of the next dipole.

Taking an invariant transverse beam emittance of  $\epsilon \cdot \beta \gamma = 30\pi \cdot 10^{-6}$  rad m and  $\beta_v = \beta_H = 2.5$  m at the target which can still be realized with standard gradient quadrupoles, we calculate a spot of 0.30 mm radius (two standard deviations in the gaussian approximation). The focus has to be made a chromatic in order to avoid additional contributions from the relatively large momentum spread.

It has been calculated that  $5 \times 10^{13}/12 = 4.16 \times 10^{12}$  particles is about the maximum beam intensity which can be concentrated on a tungsten target of special construction. Substantially higher beam intensities would lead to destruction. Heat propagates in tungsten with a speed about 1 m/sec. Since successive pulses are ejected at 66 ms in time, we can cool the target between pulses by simple conduction.

After the target, the residual proton beam must be separated from the low-energy particles by bending and absorbed in a suitable beam dump.

### III-3. Bunch Synchronization

The antiproton bunches have the same time structure as the protons in the Main Ring and they must also fit precisely within the buckets of the Booster. This is not an entirely trivial operation. Frequencies are quantized by the requirement of integer harmonic numbers in the Main Ring and the Booster. The two frequencies are automatically

matched for particles of equal energies. However, anti-protons have an energy which is substantially lower than that of the parent protons while retaining the same time structure, and frequency shift cannot be neglected.

We propose to overcome this difficulty by increasing by one unit the harmonic number in the Booster for antiproton capture and deceleration, i.e., instead of  $h = 84$  which is the nominal value for protons, we propose to operate at  $h = 85$ . In order to make this possible, the proton and antiproton relativistic factors  $\gamma_p$  and  $\gamma_{\bar{p}}$  have to satisfy the relation:

$$\frac{1}{2\gamma_{\bar{p}}^2} - \frac{1}{2\gamma_p^2} = \frac{1}{85}$$

giving  $\gamma_{\bar{p}} = 6,518$ , corresponding to  $T_{\bar{p}} = 5.177$  GeV. This is sufficiently away from the transition energy  $\gamma_t = 5.446$  to present no complications. The area of the antiproton bunches is determined by the bucket area at 200 MeV, which is 0.0352 eV sec. At the magic energy  $T_{\bar{p}} = 5.177$  GeV, we have  $\eta = \frac{1}{\gamma_t^2} - \frac{1}{\gamma^2} = 6.43 \times 10^{-3}$ ,  $f = 0.637 \times 10^6$  Hz. For the maximum rf voltage  $eV = 700$  KeV/turn and  $\cos \phi_s = 1/2$  we calculate

$$v_s = [h\eta eV \cos \phi_s / 2\pi E]^{1/2} = 2.16 \times 10^{-3}$$

$$B = (h/2\pi) [8Af\eta/pv_s]^{1/2} = 0.122$$

$$\Delta P/P_{full} = \frac{1}{\beta} [8Af v_s / p\eta]^{1/2} = 3.0 \times 10^{-3}$$

In order to match bunches, we must increase the proton bunching factor from 0.085 to 0.122. This can be easily done by reducing the MR voltage from  $3.4 \times 10^6$  V to  $8.0 \times 10^5$  V during extraction.

#### III-4. Production and Collection of Antiprotons

The booster acceptances, after allowance for alignment errors, are taken to be

$$A_V(200 \text{ MeV}) = 40\pi \cdot 10^{-6} \text{ m rad}$$

$$A_H(200 \text{ MeV}) = 40\pi \cdot 10^{-6} \text{ m rad}$$

Acceptances must match the beam emittances at 200 MeV.

Assuming adiabatic damping during deceleration the emittances scaled to 5.2 GeV injection energy are

$$A_V(\text{inj}) = A_H(\text{inj}) = 4.0\pi \cdot 10^{-6} \text{ m rad}$$

The value of the  $\beta$  function for the antiprotons at the production target is taken to be  $\beta_V = \beta_H = .025 \text{ m}$ . The  $\bar{p}$  angular divergence is then  $\theta_V = \theta_H = 13 \text{ mrad}$ , and the solid angle accepted is  $\Omega = \pi \theta_V \theta_H = 5.3 \times 10^{-4} \text{ sterad}$ .

Inclusive  $\bar{p}$  and  $\pi^-$  production has been parametrized for the existing data in Ref. 21:

$$E \frac{d^3\sigma}{dp^3}(\bar{p}) = 0.26N [p_{\perp}^2 + 1.04]^{-4.5} (1-x_R)^7$$

$$E \frac{d^3\sigma}{dp^3}(\pi^-) = N [p_{\perp}^2 + 0.86]^{-4.5} (1-x_R)^4$$

We establish the normalization  $N$  from the data of Ref. 22 in the region  $s > 1000 \text{ GeV}^2$  where scaling holds:  $N = 10.2 \text{ mb GeV}^{-2}$ .

Also in Ref. 22 is a plot of the production ratio  $f(s) = \bar{p}/\pi^- [x=0.35, p_{\perp}=0.5 \text{ GeV}/c]$  in the range  $25 < s < 2830 \text{ GeV}^2$ . Using the cross section parametrizations we extrapolate to obtain  $f_0(s) = \bar{p}/\pi^- [x=0, p_{\perp}=0]$ . By normalizing to the saturation value  $f_0(\infty)$  in the region of scaling, we obtain the scaling parameter  $\alpha(s) = f_0(s)/f_0(\infty)$  which is plotted in Fig. 4. We then have

$$E \frac{d^3\sigma}{dp^3}(\bar{p}) = 2.65 \alpha(s) [p_{\perp}^2 + 1.04]^{-4.5} (1-x_R)^7 [\text{mb GeV}^{-2}]$$

This invariant cross section, expressed in convenient lab frame variables, is just  $(1/p^2) \frac{d^2\sigma}{d\Omega(\Delta p/p)}$ . This cross section is plotted in Fig. 5 as a function of  $\bar{p}$  momentum, for various primary proton energies. For  $p_p = 6.5 \text{ GeV}/c$ , the optimum primary proton energy is 100 GeV, and the cross section is 57 mb/sterad. The 5 cm tungsten target has an efficiency of  $\epsilon = 1/3$ . The momentum acceptance of the Booster from Sect. III-3 is  $\Delta p/p = 3.0 \times 10^{-3}$ . The  $\bar{p}$  yield is then

$$Y = \frac{N_{\bar{p}}}{N_p} = \epsilon \frac{d^2\sigma}{d\Omega(\Delta p/p)} \frac{\Omega \Delta p/p}{\sigma_{\text{tot}}} = 7.5 \times 10^{-7}$$

This result agrees within 30% with the Monte Carlo cascade calculation of Ref. 23. With  $4.6 \times 10^{13}$  protons in 12 Booster pulses in the MR, this corresponds to  $N_{\bar{p}} = 3.5 \times 10^7$ .

We have designed with some detail the critical parts of the  $\bar{p}$  collection channel. It consists of three distinct parts:

i) The collecting lens system.

It is a 6-quadrupole system consisting of an initial doublet ( $Q_1, Q_2$ ), two field-lenses ( $Q_3, Q_4$ ) and a final matching doublet. The quadrupole dimensions and gradients are listed in Table II. We show in Fig. 6 trajectories of off-momentum particles and several limiting rays.

ii) A momentum matching section. This section separates the antiprotons from the main proton beam and matches dispersion of the beam to the requirements of the Booster.

iii) Injection into the Booster. Here we can use the new extraction system to be installed in straight section 3 (see Fig. 7). Although the detailed design is only now in progress, it is well within present technology and we anticipate no major problems.

#### IV. ANTIPROTON STORAGE AND COOLING

##### IV-1. Design Criteria.

Antiprotons are transferred to a 200 MeV storage ring (Freezer Ring) where cooling and repetitive accumulation takes place.

We suggest a very simple lattice and reduced periodicity. The central requirement of the lattice is a good acceptance and adequate long straight sections for electron cooling. The major goal is to design a lattice with a minimum number of dipoles and quadrupoles that gives the longest good quality straight sections. We present here one example of a lattice which approximately satisfies these criteria. The basic lattice has 12 cells, 24 dipoles, and 36 quadrupoles. Figure 8 shows a unit cell and the resulting betatron functions. The machine parameters and performance are given in Table III. A large acceptance is obtained that is well matched to the booster or to the Fermilab linac should the Freezer be used as a proton cooler or for multiturn linac injection (see Appendix III).

We would like to preserve the possibility of transferring synchronously to the Freezer. This places a constraint on the circumference of the Freezer, since in order to match harmonics with the Booster we have

$$\frac{h_F}{85} = \frac{C \times 13.25}{2\pi \times 10^3 \text{m.}}$$

The choice  $h_F = 86$  yields  $C = 479.78 \text{m}$ , which fits comfortably in the Booster tunnel (see Figure 9 and 10).

When we return the cooled and stacked anti-protons to the

Booster for reacceleration and injection in the MR, it is necessary to do so with  $h = 84$  in the Booster. This dictates  $h_F = 85$ . This corresponds to a circumference  $C = 479.85\text{m}$ , negligibly different from that for injection to the Freezer.

The transfer of the  $\bar{p}$  beam from the Booster to the Freezer has to have sufficient aperture to accommodate the full Booster beam acceptance. This can be achieved using a fast kicker  $B_1$  in long straight 7, followed by a pulsed current septum  $B_2$  in long straight 6. These elements are described in Table II. A second, identical pair of elements are then used in reverse sequence in the Freezer ring for injection.

The transfer from the Freezer into the Booster is accomplished at straight 5 with a more modest version of  $B_1, B_2$ , since the aperture requirement is now minimal.

We find that because of the rise and decay times of the full aperture kickers which are necessary to extract and inject the relatively large beam, as many as 3 bunches corresponding to 100 nsec may be lost in the transfer process.

#### IV-2. Magnetic Structure

There are several possible designs for the bending and quadrupole magnets that form the building blocks of the Freezer lattice. The bend can be either a window-frame or H design; the quadrupole can be either a standard design with iron pole tips, or a Panofsky quad formed by a box of 4 alternating current sheets. We are presently evaluating each design in regard to the required field quality and cost.

For the bending magnet, we have examined a number of existing

designs (Fermilab 10' EPB dipole, SLAC 18D72, ANL BM105, 107, 109, 110, 114). It seems in general that the fraction  $\epsilon$  of horizontal "good field" aperture to physical aperture is  $\epsilon \sim (1+2\alpha)^{-1}$  in a good design of either an H or window frame, where  $\alpha$  is the ratio of vertical/horizontal aperture in the desired good field region. For the case discussed here  $\epsilon = 0.5$ . The field quality in the window frame is, however, sensitive to coil placement, and places rather stringent demand on the fabrication process. This also potentially produces significant variations in multipole moments from one magnet to another. For the design case presented here, we use a scaled replica of the 10' EPB H dipole, shown in Fig. 11.

One question that arises in the context of the bending magnets is what guide field should be used. Three considerations arise in this connection. First, the field quality of a dipole below a few kG suffers from the variation of Fe magnetization at low field. Second, the sagitta for a magnet of given bending angle decreases as guide field increases. The sagitta  $\delta$  [m] of particles of momentum  $p$  [GeV] in a magnet of field  $B$  [T], bend angle  $\phi$  [rad] is

$$\delta = \frac{p\phi^2}{2.4B}$$

Thus for a fixed number of bends (fixed  $\phi$ ), sagitta is minimized for maximum  $B$ . Third, as will be discussed in the next section it seems desirable to locate a distributed ion pump system in the fringe field of the dipoles. An optimized design of such a system improves in pumping speed up to a field of ~4kG. We have tentatively chosen for this design a guide field of 5kG, corresponding to 24 m dipoles.

For the quadrupoles, there exist 21 quadrupoles that previously

formed the muon channel of the Chicago synchrocyclotron. The design is shown in Fig. 12. We are examining their suitability for the Freezer ring. Several Panofsky quads have been built at Cornell.<sup>25</sup> The Panofsky design is problematic for a storage ring for the same reasons as a window frame dipole. Additionally, its power requirements are greater for a given gradient than for a standard quad.

The parameters of both magnets are given in Table IV.

#### IV-3. Long Straight Sections for Electron Cooling

In order to obtain rapid cooling of the beam it is desirable that the  $\bar{p}$  beam have a small divergence in the straight section. This requirement can be met by having  $\beta_H, \beta_V$  large in the straight section. We have achieved one simple design of such a straight section using two quadrupole triplets that match well the basic cell described before. The horizontal acceptance remains  $\sim 100\pi$  m and 8" bore quadrupoles are adequate for the triplets. The  $\beta_V, \beta_H$  are in the range of 15-40 m leading to an angular divergence of  $\sim (1-2)\text{mr}$ . The p function (off momentum function) goes to  $1\div 2\text{m}$  in the same straight section. We suggest that the cooling straight sections be instrumented in this way whereas the other straight sections need fewer quads ( $\sim 2$  doublets, incorporating the D quads of the regular cells).

#### IV-4. Vacuum System

The Freezer ring must be capable of storing an antiproton beam for a time of the order of a day without serious losses due to beam-gas scattering. We will examine the vacuum requirements implied and discuss one attractive approach to meeting them.

Beam growth occurs by Coulomb scattering from gas molecules, and beam loss occurs each time an antiproton collides with a gas nucleus. The rate of increase in the mean square of the projected angle of Coulomb scattering is:<sup>26</sup>

$$\frac{d\langle\phi^2\rangle}{dt} = \frac{4\pi r_p^2 c}{\beta^3 \gamma^2} \sum_i n_i Z_i^2 \ln 38360 / \sqrt{A_i Z_i}$$

where  $r_p = 1.54 \times 10^{-16}$  cm the proton radius,  $n_i$  is the density and  $Z_i$  and  $A_i$  are the atomic number and atomic weight of atoms of type  $i$ . Snowdon<sup>27</sup> has analyzed the residual gas composition in the MR at a pressure of 0.21  $\mu$  Torr. We will assume the same composition in the Freezer, and follow here his calculation of beam growth. The angular growth is

$$\frac{1}{p} \frac{d\langle\phi^2\rangle}{dt} = 0.25 \text{ rad}^2 \text{ sec}^{-1} \text{ Torr}^{-1}$$

The diffusion rate of the quantity  $W = (dy/d\theta)^2 + v^2 y^2$  is  $D = R^2 d\langle\phi^2\rangle/dt$  where  $y$  is the amplitude of betatron motion,  $v \sim 4$  is the tune, and  $R = 75$  m is the average radius. The beam lifetime is<sup>28</sup>

$$\tau = \frac{1}{D} \left( \frac{2va}{2.4} \right)^2$$

where  $a = 1$  cm is the tolerable aperture growth. The lifetime against Coulomb scattering is then  $\tau$  [sec] =  $8.0 \times 10^{-7} / p$  [Torr]

A lifetime of one hour requires a mean pressure of  $2 \times 10^{-10}$  Torr.

Clearly we must rely on electron cooling to damp the growth of the stack.

The fraction  $f$  of beam removed by nuclear collisions with gas is

$$df/dt = \beta c \sigma_{pp} \sum_i n_i A_i$$

where  $\sigma_{p\bar{p}} = 170$  mb is the  $p\bar{p}$  total cross-section at 650 MeV/c.

$$\frac{1}{P} \sum n_i A_i^{2/3} = 1.5 \times 10^{17} \text{cm}^{-3} \text{Torr}^{-1},$$

$$\tau \text{ [sec]} = 2.3 \times 10^{-3} / P \text{ [Torr]}$$

A lifetime of one day requires a mean pressure of  $2.5 \times 10^{-8}$  Torr.

The vacuum in the Freezer should thus be  $\leq 10^{-10}$  Torr. One appealing approach to achieving this in the bending lattice is to locate a distributed ion pump system in the fringe field of the dipoles.<sup>24</sup> Rowe and Winter<sup>29</sup> estimate a pumping speed of 1600  $\mu$ /sec from each 1m dipole so equipped. The cost is about 1/2 that of a standard ion pump of capacity 500  $\mu$ /sec. Standard ion pumps would still be required in the straight sections. The conductance of a 5m section of the Freezer vacuum pipe is approximately 22  $\mu$ /sec.

#### IV-5. Electron Cooling

The Novosibirsk group has demonstrated that low-momentum proton beams can be "cooled" to very small transverse dimensions and very small momentum spread.<sup>3</sup> The basic idea is that the transverse and longitudinal oscillations of the proton beam are transferred by Coulomb scattering to an electron beam that is injected in one of the straight sections of the storage ring. For maximum cooling efficiency the velocity of the  $\bar{p}$  and of the  $e^-$  should be the same ( $\beta_{\bar{p}} = \beta_e$ ), since the Coulomb scattering cross section will be a maximum. Their results will be used to extrapolate the cooling rates expected in our case.

We assume the entire Booster beam is transferred in one turn at 200 MeV into the Freezer Ring. The emittances of the beam

at this stage are  $A_V = A_H = 40\pi \cdot 10^{-6} \text{ m}$ .  $\Delta p = 1.3 \text{ MeV/c}$ . The beam is assumed to be adiabatically debunched either in the Booster or in the Freezer. In the cooling points ( $\beta_V = \beta_H = 15\text{m}$ ) the half-beam sizes are as follows:

$$W_\beta = \sqrt{A_H \beta / \pi} = 2.5 \text{ cm} \quad W_{\Delta p} = \chi_p \cdot \frac{\Delta p}{p} = 0.4 \text{ cm}$$

$$h = \sqrt{A_V \beta / \pi} = 2.5 \text{ cm}$$

The total area is then  $A = \pi (W_\beta + W_{\Delta p}) \cdot h = 23 \text{ cm}^2$ .

Angular divergencies are also of interest. They are

$$\theta_H = \sqrt{A_H / \beta \pi} = 1.6 \text{ mrad}$$

$$\theta_V = \sqrt{A_V / \beta \pi} = 1.6 \text{ mrad}$$

which are, as we shall see, quite comparable to the angles of the electron beam.

An approximate formula for the cooling time for a parallel  $e^-$  and  $p$  (or  $\bar{p}$ ) beam is given by ( $\theta_e \ll \theta_p^-$ )

$$\tau = .05 \left( \frac{M_p^-}{m_{e^-}} \right) \frac{\gamma_p^-^5 \beta_p^-^3 \theta_p^-^3}{n_e r_e^2 c L \eta \ln(\theta_p^- / \theta_e)}$$

This formula reduces to

$$\tau = \frac{1.2 \times 10^7 \gamma^5 \beta^4 \theta_p^3}{j_e \eta \ln(\theta_p / \theta_e)} = \frac{2.5 \times 10^6 \theta_p^3}{j_e \eta}$$

where  $\tau$  = end-point cooling time [sec]

$j_e$  = electron beam current density [ $A/cm^2$ ]

$r_e$  = classical electron radius [cm]

$n_e$  = electron beam density [ $cm^{-3}$ ]

$\theta_p^-$  =  $\bar{p}$  beam divergence [rad]

$\gamma = E_p^-/m_p^-$ ,  $\beta_p^- = (P_p^-/E_p^-)$

$\eta$  = cooling length/total circumference of cooling ring

$L$  = Coulomb logarithm = 15

In the approximation  $\theta_e \gg \theta_p$ , the formula will contain the factor  $\theta_e^3$  instead of  $\theta_p^3$ .

The latest experimental results from Novosibirsk are as follows:

Proton energy	65 MeV
Electron energy	35 keV
Cathode diameter of the electron gun	20 mm
Electron current $I_e$	0.1 - 0.8 A
Proton current $I_p$	20 - 100 $\mu A$
Average vacuum	$5 \times 10^{-10}$ Torr
Equilibrium size (diameter) of the proton beam in the middle of the section	0.47 mm
Cooling Time ( $I_e = 0.8A$ ) $\tau_e$	83 msec
Proton life time in the cooling regime	more than 8 hours
Angular divergence of electrons	$\theta_e \approx 3$ mrad
Specific flux of neutral hydrogen atoms ( $\frac{dN}{dt}/I_e I_p$ )	$80 A^{-1} \mu A^{-1} sec^{-1}$

In order to extrapolate to our situation, we must take into account the following factors:

(i) The kinetic energy is higher, 200 MeV instead of 65 MeV. According to the  $\gamma^5 \beta^4$  scaling law, this increases the cooling time by a factor 10.8.

(ii) The angular divergence of the electron beam which dominates with respect to that of the (anti) proton in both cases is given by the formula discussed in Appendix II:

$$\tau = \frac{V}{\dot{z}} = 0.102 \frac{I}{BVr_0}$$

For our case,  $r_0 = 2.5$  cm,  $V = 1.1 \times 10^5$  V,  $B = 0.2$  T, and  $I = 23$  A. Comparing it with Budker's case, we can see that electron temperatures are expected to be comparable. Hence, the factor is the same for both cases.

(iii) The fraction of circumference with electron beams was  $\eta = 0.016$  for Budker and it is  $\eta = 0.063$  for us. This decreases the cooling time by a factor 4.

A detailed comparison between the Novosibirsk and Fermilab situations is summarized in the following table:

		<u>Novosibirsk</u>	<u>Fermilab</u>
Proton energy	T	65	200 MeV
Electron energy	T <sub>e</sub>	35	110 keV
Electron current	I <sub>e</sub>	0.8	23A
Proton current	I <sub>p</sub>	100	3 $\mu$ A
Electron beam radius	r <sub>e</sub>	1	2.5 cm
Fraction of circumference cooled	$\eta$	0.016	0.06
Angular electron spread	$\theta_e$	3.0	3.0 mrad
Proton angular spread	$\theta_p$	-	1.6 mrad
Cooling time	sec	0.086	0.0466 (*)

(\*) Extrapolated using the dependence

$$\tau \sim \gamma^5 \beta^4 \theta^3 / \eta j_e, \text{ where } j_e = I_e / \pi r_e^2$$

We remark that the cooling time is expected to be appreciably shorter than necessary.

In the above table, the space charge of the electron beams lead to a tune shift of about .25 in both transverse dimensions. Although this may seem large, it should be noted that the electron density must, in any case, be very uniform so the tune spread will be small and correction, if necessary, can be straightforward. The half integral stopbands caused by the electron beam can be cancelled by proper periodicity of the cooling regions in the cooling ring.

#### IV-6. Electron Beam and Electron Gun

We propose that a total of at least 30m of cooling length be incorporated into the machine. The electron beam must be maintained parallel over 10m length. Space charge effects will blow up the electron beam unless a solenoidal magnetic field is maintained over the entire length of cooling. Furthermore, as discussed in Appendix II, the magnetic field lines must be shaped and carried all the way back into the electron gun cathode. The electrons, after exiting the cooling section, are to be decelerated to regain the large energy in the beam. The system is shown schematically in Fig. 13.

The accelerating voltage must be 110 kV, equivalent to a beam power of 2.5 MW. Assuming a 98% efficiency of recovery, we have a dissipation of 50kW/beam or a total of 200kW, which is acceptable.

The electron current requirement is about  $1 \text{ A/cm}^2$  over approximately  $10 \text{ cm}^2$  at 110 KeV energy. CW electron guns have been constructed that give this performance. For example, one such gun is shown in Fig. 14, that is to be used in PEP. This gun gives  $\sim 23\text{A}$  of current for a voltage of 110 keV over an area of approximately  $18 \text{ cm}^2$ .

#### IV-7. Stacking in the Freezer

Two techniques are used for stacking in the Freezer. Electron cooling can be used to move the beam and therefore to remove the antiprotons from the injection area after the previous Booster capture has been cooled. This motion is slow, and a more efficient technique will be needed to move each booster capture into a preliminary stack that will contain all 12 captures. For this purpose, rf stacking is to be used. During the time that the Booster is being filled with protons and the protons accelerated in the Main Ring, a modest rf will be used to adiabatically capture the newly-cooled beam. This can be done without disturbing the cool beam already present at the inner edge of the aperture. The new beam is then moved over to the stack and stacked next to it. This procedure is shown schematically in Fig. 15.

## V $\bar{p}p$ COLLISIONS IN THE MAIN RING

The accumulation cycle for collecting antiprotons from a full MR pulse requires a time of  $\sim 3$  sec. We estimate a yield of  $3.7 \times 10^7$  antiprotons per cycle, based on a MR filling of  $5 \times 10^{13}$  protons. The cooled  $\bar{p}$  stack then has  $4.5 \times 10^{10}$   $\bar{p}$ 's after one hour of accumulation.

Extraction at 8 GeV is done in booster straight section 8, following a pulse of the fast kicker  $B_1$  in long straight 9. Again, aperture requirement is minimal, and the existing spare extraction septum can be used. The 8 GeV  $\bar{p}$ 's then are bent through an arc and enter the transfer line for 8-GeV reverse injection to the main ring.

We assume that these antiprotons are now injected into the MR together with  $4 \times 10^{12}$  protons, so that the MR now contains two counter-circulating beams of 84 RF buckets (one Booster pulse) each. The beams are accelerated synchronously to 150 GeV/c.

The luminosity at a collision site is then

$$\mathcal{L} = \frac{N_1 N_2 f}{2\pi \sqrt{\sigma_{x1}^2 + \sigma_{x2}^2} \sqrt{\sigma_{y1}^2 + \sigma_{y2}^2} N_B}$$

where  $N_1$  and  $N_2$  are the number of protons and antiprotons,  $N_B=84$  is the number of buckets in each beam, and  $f=47$  kHz is the MR revolution frequency. The (Gaussian) beam sizes are obtained under the assumptions:

$$\sigma_{x2} \ll \sigma_{x1}, \quad \sigma_{y2} \ll \sigma_{y1}, \quad \sigma_{x1} = \sigma_{y1} = \sigma$$

The emittance of a Main Ring proton beam is  $\epsilon = 6\pi\sigma^2/\beta^* = \epsilon_0/\gamma$  where  $\epsilon_0 \approx 20\pi \cdot 10^{-6} \text{ m}$  is the invariant emittance of the present Main Ring beam, and  $\beta^* = 2.5 \text{ m}$  is the local  $\beta$  in the intersect.<sup>30</sup>

$$\mathcal{L} = \frac{3N_1 N_2 f \gamma}{\epsilon_0 \beta N_B} = 3.0 \times 10^{28} \text{ cm}^{-2} \text{ sec}^{-1}$$

Thus a luminosity of  $10^{29} \text{ cm}^{-2} \text{ sec}^{-1}$  can be obtained in  $\sim 3$  hours of  $\bar{p}$  accumulation.

## VI $\bar{p}$ BEAM REGENERATION

We can estimate the  $\bar{p}$  beam lifetime in the Main Ring as in Section IV-6. The mean Main Ring vacuum is  $\sim 5 \times 10^{-7}$  Torr. The beam loss due to nuclear collisions gives a lifetime of 2.7 hours. After this time, we must begin again the  $\bar{p}$  accumulation process.

We also estimate the beam growth due to Coulomb collisions. The proton beam size is  $\sigma = \sqrt{\beta_{av} \epsilon_0 / 6\pi\gamma} = 1.2\text{mm}$  for  $\beta_{av} = 70\text{m}$ . Thus, luminosity will decrease by a factor  $\sim 2$  for a beam growth of 1mm, and quickly thereafter. The Coulomb lifetime for 1mm growth is then 190 sec.

Clearly a major concern for implementing  $\bar{p}p$  colliding beams will be the possibility of improving the present Main Ring vacuum. We are advised that it may be possible to reduce the vacuum by a factor 5  $\div$  10 before being limited by conductance or basic design.

In any case, it will be desirable to regenerate the  $\bar{p}$  beam using electron cooling to compensate for the growth from Coulomb scattering. The most straightforward way of accomplishing this is to dump the  $p$  beam and decelerate the  $\bar{p}$ 's to 8 GeV/c, then transfer them to the Booster through the existing injection system and transfer tunnel. After deceleration in the Booster, they would be re-cooled in the Freezer and the cycle repeated.

## VII. CONCLUSIONS

We believe that the possibility of implementing, at modest cost,  $\bar{p}p$  colliding beams at Fermilab in the near future is established. The direct study of electron cooling at Fermilab is a high initial priority. The physics of high energy  $\bar{p}p$  colliding beams has definite advantages for the observation of many conceivable new phenomena. This is especially true for processes that involve parton-antiparton collisions, where the rates will be maximal and the background due to parton-parton collisions minimal.  $\bar{p}p$  colliding beams of luminosity  $10^{29} \text{ cm}^{-2} \text{ sec}^{-1}$  can be obtained and are adequate to observe exciting phenomena such as W production. Finally, the construction of a realistic electron cooling device at Fermilab is likely to have a large impact on accelerator development in the United States for years to come. Each of these reasons is sufficient motivation for this project; in total we believe they provide a compelling necessity.

### ACKNOWLEDGEMENTS

We gratefully acknowledge the contributions of A. Ruggiero to the evolution of this project. We also thank M. Barton, T. Collins, E. Courant, C. Curtis, D. Edwards, H. Edwards, R. Huson, D. Johnson, R. Johnson, J. Laslett, M. Lebacque, P. Livdahl, J. LoSecco, S. Snowdon, L. Teng, R.R. Wilson, D. Winn, and W. Winter for helpful discussion. Special thanks are due to E. Rowe and W. Trzeciak for lattice design.

References

1. C. Rubbia, P. McIntyre and D. Cline, Producing the Massive Intermediate Vector Meson with Existing Accelerators, submitted to Phys. Rev. Letters, March 1976.
2. D. Cline and C. Rubbia, "Energy Doubler at FNAL as a High Luminosity  $p\bar{p}$  Storage Ring Facility." Report in preparation.
3. G. I. Budker, Atomic Energy 22, 346 (1967); G. I. Budker, et al: "Experimental Facility for Electron Cooling," BNL-TR-588 (1974); "Preliminary Experiments on Electron Cooling," BNL-TR-593 (1974); "Experimental Study of Electron Cooling," BNL-TR-635 (1976).
4. S. Van der Meer, CERN-ISR-PS/72-31, August, 1972 (unpublished).
5. D. Cline, P. McIntyre, and C. Rubbia, "Proposal to Construct an Antiproton Source for the Fermilab Accelerator," Fermilab Proposal Number 492 (1976).
6. G. I. Budker, et al., "New Results of Electron Cooling Studies," preprint submitted to Nat. USSR Conf. on High Energy Accelerators (Dubna) Oct. 2, 1976.
7. The possibility of using the Booster accelerator for phase-space cooling has been remarked at informal meeting by ourselves, D. Berley, and R. Johnson.
8. F. J. Hasert, et al., and A. Benvenuti et al., papers submitted to the Sixth International Symposium, Bonn (1973); F. J. Hasert et al., Phys. Letters 46B, 138 (1973); A. Benvenuti et al., Phys. Rev. Letters 32, 800 (1974).
9. U. Camerini, D. Cline, W. Fry and W. Powell, Phys. Rev. Letters 13, 318 (1964); M. Bott-Bodenhausen et al., Phys. Letters 24B, 194 (1967).
10. S. L. Glashow, J. Iliopoulos and L. Maiani, Phys. Rev. D2, 1285, 1970.
11. B. Aubert et al., "Experimental Observation of  $\mu^+\mu^-$  Pairs Produced by Very High Energy Neutrinos," in Proceedings of the Seventeenth International Conference on High Energy Physics, London, 1974 and in Neutrinos - 1974, AIP Conference Proceedings No. 22, edited by C. Baltay (American Institute of Physics, New York, 1974), p. 201. A. Benvenuit et al., Phys. Rev. Letters 34, 419 (1975), *ibid.* 34, 597 (1975), J. J. Aubert et al., Phys. Rev. Letters 23, 1404 (1974), and J. E. Augustin et al., Phys. Rev. Letters 23, 1406 (1974).
12. J. von Krogh et al., Phys. Rev. Letters 36, 710 (1976); J. Blietschau et al., Phys Letters 60B, 207 (1976).
13. J. J. Aubert et al., Phys. Rev. Letters 33, 1404 (1974); J. E. Augustin et al., Phys. Rev. Letters 33, 1406 (1974).

References (Continued)

14. S. Weinberg, Phys. Rev. Letters 19, 1264 (1967), and A. Salam in Elementary Particle Physics (edited by N. Svortholm. Almquist and Wiksells, Stockholm, 1968), p. 367.
15. L. Okun and M. Voloshin, "Production of Intermediate Bosons in pp and pp Collisions," Preprint ITEP-III, 1976. Many informal calculations have been made by several authors.
16. J. D. Bjorken, Report at the 1976 SLAC Summer School.
17. A. Benevenuti et al., "Test of Locality of the Weak Interaction in High Energy Neutrino Collisions," submitted to Phys. Rev. Letters (March, 1976).
18. T. K. Gaisser, F. Halzen and E. A. Paschos, "Hadronic Production of Narrow Vector Mesons," BNL preprint 21489.
19. Booster Synchrotron, Fermilab TM-405, edited by E.L. Hubbard (1973).
20. F. Mills, private communication.
21. D. Carey et al., "Unified Description of Single-Particle Production in p-p Collisions," NAL-Pub-74/49-THY/EXP.
22. M. G. Albrow et al., "Negative Particle Production in the Fragmentation Region at the CERN ISR," Nucl. Phys. (1973).
23. B. Chirikov, V. Tayursky, H. Mohring, J. Ranft and V. Schirrmeister, "Optimization of Antiproton Fluxes from Targets Using Hadron Cascade Calculations," KMU-HEP 7606 (preprint), March 1976.
24. Cummings et al., "Vacuum Systems for SPEAR," SLAC-Pub-797.
25. M. Tigner, private communication.
26. B. Rossi, "High Energy Particles," Prentice-Hall, New Jersey, 1952.
27. S. Snowdon, "Residual Gas Analysis in Main Ring to Obtain Mean-Square Scattering Angle and Beam Lifetime," Fermilab TM-341.
28. L. C. Teng, Accelerator Experiment Note (1/11/72) Fermilab.
29. E. Rowe and W. Winter, private communication.
30. T. Collins, "Easy Low  $\beta$  for the Main Ring," TM-649, March 11, 1976.

## Appendices

### Appendix I      Initial Experimental Test of Electron Cooling - Racetrack Ring Set Up On the Surface

While electron cooling has been experimentally demonstrated, it is far from well established for the high current-large divergence antiproton beam proposed here. While the simple theoretical estimates give rapid cooling times as discussed in 6b, it is of great importance to have detailed measurements of the cooling phenomena. Setting up the Freezer ring in the booster tunnel would limit the experimental measurements since the booster is constantly in use. It is therefore proposed that the same magnetic structure, but with only two long straight sections (Racetrack), be initially assembled on the surface at Fermilab near the linac so that a 200 MeV proton beam is available for cooling studies.

The 12 period lattice described in 5a can be abbreviated using the same elements, as shown in Fig. 17. The overall size then becomes  $25 \times 40 \text{ m}^2$ . There is of course a saving in the number of quadrupoles needed for the ring as well as the length of vacuum pipe needed. One or both of the long straight sections should be instrumented for electron cooling as described in 6c. These cooling studies and studies of the performance of the storage ring will be invaluable for the operation of the Freezer in the booster tunnel.

Appendix II Theory of Electron Confinements in a Magnetic Field

In order to damp betatron oscillations and momentum spread of a proton or antiproton beam in a storage ring, Budker has proposed to make it interact with a strong current of almost parallel electrons travelling with the same average speed as the beam. In the practical realization of such larger currents, space charge effects must be taken into account. A simple way of compensating for the divergence due to space charge forces consists of sending electrons along the axis of a uniform solenoidal magnetic field.<sup>2</sup>

Brillouin<sup>3</sup> has investigated the conditions in which stable cylindrical electron beams could be produced. His work has been extended by other authors.<sup>4,5</sup> Unfortunately, as we shall see, the Brillouin solution cannot be applied to our case, since it implies a too large difference in velocity between peripheral electrons and paraxial electrons. Instead of magnetically focussed flow, we must operate in the limiting condition of magnetically confined flow. The main effect of increasing the field is the one of producing periodic scallops on the beam. These scallops are very small and affect only very slightly the beam shape.

We shall start with a review of the theory of confined electron beam.<sup>6</sup>

## 2. Bush's theorem.

Let us define a frame of polar coordinates,  $r$ ,  $\theta$  and  $z$  as shown in Figure 16. The Bush theorem gives the angular velocity of an electron in which neither the electric nor the magnetic field has component in the  $\theta$  direction. This is obviously the most general case for an axially symmetric set-up.

The Lorentz force equation can be written as:

$$\ddot{r} - r\dot{\theta}^2 = -\eta(E_r + B_z r\dot{\theta}) \quad (1)$$

$$\frac{1}{r} \frac{d}{dt} (r^2 \dot{\theta}) = -\eta(-B_z \dot{r} + B_r \dot{z}) \quad (2)$$

$$\ddot{z} = -\eta(E_z - B_z r\dot{\theta}). \quad (3)$$

where  $\eta = e/m = 1.76$  coulombs/kg.

From the expression  $\nabla \cdot B = 0$ , we get  $B_r = (-r/2) \frac{\partial B_z}{\partial z}$  and remembering that  $\frac{d}{dt} = \dot{r} \frac{\partial}{\partial r} + \dot{z} \frac{\partial}{\partial z}$  we can interpret Eq. (2) to give

$$r^2 \dot{\theta} = \eta \int (B_z r \dot{r} + \frac{r^2 \dot{z}}{2} \frac{\partial B_z}{\partial z}) dt = \eta \frac{B_z r^2}{2} + c.$$

The initial constant can be related to the cathode conditions  $r = r_0$ ,  $\dot{\theta} = 0$  and  $B_z = B_0$ . Then:

$$r^2 \dot{\theta} = \frac{\eta}{2} (B_z r^2 - B_0 r_0^2). \quad (4)$$

Using the Larmor angular frequency  $\omega_L = \eta \frac{B_z}{2}$  and putting  $\omega_0 = \eta \frac{B_0}{2}$  we can rewrite the (4) as

$$\dot{\theta} = \omega_L - \omega_0^2 \left(\frac{r_0}{r}\right)^2. \quad (5)$$

Equation (5) is known as Bush's theorem.

### 3. Brillouin flow.

Inserting the Equation (5) in Equation (1) we obtain:

$$\ddot{r} = -\eta E_r + r \left( \omega_0^2 \frac{r_0^4}{r^4} - \omega_L^2 \right). \quad (6)$$

From the Gauss's theorem for a uniform cylindrical beam of current  $I_0$ ,  $E_r = -I_0 / 2\pi\epsilon_0 u_0 r$ , and therefore:

$$\ddot{r} = \frac{\eta I_0}{2\pi\epsilon_0 u_0 r} + r \left( \frac{\omega_0^2 r_0^4}{r^4} - \omega_L^2 \right). \quad (7)$$

From Eq. (7) one can see that the magnetic field is most effective when  $\omega_0 = 0$ , i.e., the cathode is outside the field. For a cylindrical beam, obviously  $\ddot{r} = 0$ , which gives

$$B_B^2 = \frac{2I_0}{\pi\eta\epsilon_0 u_0 r^2} = \frac{2\omega_p^2}{\eta^2} = \frac{\sqrt{2} I_0}{\pi\eta^{3/2} \epsilon_0 r^2 V_a^{1/2}}$$

$$= 7.0 \times 10^{-7} I_0 / V_a^{1/2} r^2. \quad (8)$$

where  $B_B$  is the Brillouin field value. From Eq. (5) we see that  $\dot{\theta}_B = \omega_L$ , when  $\omega_0 = 0$ . Electrons then pivot about the z axis with Larmor's angular frequency. One can easily show that the Brillouin's condition is equivalent to balancing the centrifugal force and the electrostatic force with the magnetic force.<sup>6</sup>

From Eq. (7) we can derive the result

$$-\eta E_r = r \dot{\theta}_B^2 = \frac{\partial V}{\partial r} \eta$$

or, by integration, since  $\dot{\theta}_B^2 = \text{const}$ :

$$V = V_a + \frac{r^2 \dot{\theta}_B^2}{2\eta}$$

The electrons at the periphery then have a larger energy than the one at the center of the beam. By equating kinetic and potential energies we get

$$(\dot{z})^2 + (r\dot{\theta})^2 = 2\eta V = 2\eta V_a + r^2 \dot{\theta}_B^2.$$

from which we get

$$\dot{z} = u_0 = \sqrt{2\eta V_a}$$

which means that all electrons have the same longitudinal velocity, corresponding to the potential along the axis.

The transverse velocity at the periphery is

$$r\dot{\theta}_B = r\omega_L$$

Let us consider a practical example. Assume  $\frac{I_0}{\pi r^2} = 10^4$  A/m<sup>2</sup> and  $V_a = 5 \times 10^4$  volt. From Eq.(8) we get  $B_B = 55.95 \times 10^{-4}$  Tesla. The Larmor frequency is  $\omega_L = 432$  Mc/s, giving a radial velocity  $r\omega_L = 4.92 \times 10^6$  m/sec already at  $r = 1$  cm, to be compared to  $\dot{z} = 1.237 \times 10^8$  m/s. This corresponds to about 40 mrad max angular spread of the electron beam of 1 cm radius, and it is much too large to be acceptable. Therefore, the Brillouin flow is not useful to our application.

#### 4. "Brute force" confinement

We try next to make the magnetic field strong enough to restrict the transverse motion to an acceptable amount.

Suppose we have a disk cathode of radius  $r_0$  normal to a strong magnetic field  $B$  in the  $z$  direction. We shall assume that the cathode is the same as at any plane along the beam. This solution is very attractive for its simplicity as long as the cathode has sufficiently large emission density. Those sophisticated forms of confined flow will be considered at the end. Equation (7) becomes:

$$\ddot{r} = \eta \frac{\partial V}{\partial r} + r\eta^2 \frac{B_z^2}{4} \left( \frac{r_0^4}{r^4} - 1 \right).$$

The paths of the peripheral electrons are helices and the beam assumes a scalloped form. At the equilibrium radius  $r_m, \ddot{r} = 0$ . inserting  $\frac{\partial V}{\partial r}$  from Gauss's law we get:

$$1 - \left( \frac{r_o}{r_m} \right)^4 = \frac{\sqrt{2} I_o}{\pi \epsilon_o \eta^{3/2} B_z^2 V^{1/2} r_m^2} \quad (9)$$

Therefore, increasing B, gives  $r_m \rightarrow r_o$ . According to Pierce<sup>6</sup> we can define

$$K = \frac{I_o}{\sqrt{2} \pi \epsilon_o \eta^{3/2} B_z^2 V^{1/2} r_o^2} = 3.5 \times 10^{-7} \frac{I_o}{B_z^2 V^{1/2} r_o^2} \quad (10)$$

and Eq. (9) becomes

$$\left( \frac{r_m}{r_o} \right)^4 - 2K \left( \frac{r_m}{r_o} \right)^2 - 1 = 0$$

or

$$r_m = r_o \left[ \sqrt{(K^2 + 1)} + K \right]^{1/2} \quad (11)$$

It is interesting at this point to evaluate K for the typical case  $B_z = 0.1$  Tesla,  $I_o/\pi r^2 = 10^4$  A/m<sup>2</sup> and  $V = 5 \times 10^4$  V. Inserting numerical values, we get  $K = 3.9 \times 10^{-4}$ . Hence, the approximation  $K \ll 1$  is solid since one can approximately write:

$$r_m \cong r_o \left( 1 + \frac{K}{2} \right) \quad (12)$$

We proceed next to the investigation of the ripple on the beam i.e. the motion around  $r_m$ . To do this we use the method of Kleen and Pösche<sup>7</sup>. We put

$$r(t) = r_m [1 + \delta(t)] \quad (13)$$

Since  $\delta$  is small, we expand  $r^{-1}$  and  $r^{-3}$  by the binomial theorem.

With these substitutions in Eq. (7) we get

$$\frac{d^2 \delta}{dt^2} + 2 \left( 1 + \frac{r_o^4}{r_m^4} \right) \omega_L^2 \delta = 0 \quad (14)$$

which is the classic harmonic oscillator solution for an angular frequency.

for an angular frequency  $\tilde{\omega} = \sqrt{2 \left( 1 + \left( \frac{r_0}{r_m} \right)^4 \right)} \omega_L \approx 2\omega_L$ :

$$\delta = c_1 \cos(\tilde{\omega}t) + c_2 \sin(\tilde{\omega}t)$$

At the cathode  $t=0$  and  $r=r_0$  or  $r_0=r_m(1-\delta)$ ;

$$\delta = \left( 1 - \frac{r_0}{r_m} \right) \cos(\tilde{\omega}t) \quad (15)$$

The maximum ring diameter is then  $z$  or,

$$r_m \left( 2 - \frac{r_0}{r_m} \right) = r_m \left( 1 + \frac{K}{2} \right) = r_0 \left( 1 + \frac{K}{2} \right)^2$$

Since the minimum is  $r_0$ , the ratio of maximum to minimum is  $(1 + K/2)^2$ . This is an extremely small variation since for our numerical case  $K = 3.3 \times 10^{-4}$ .

The angular speed  $\hat{\theta}$  can be easily described from the Bush's theorem:

$$\hat{\theta} = \omega_L \left( 1 - \frac{r_0^2}{r^2} \right) \quad (16)$$

The radial speed  $r$  is in turn calculated confirming Eq.(13) and Eq.(15).

$$\dot{r} = \tilde{\omega} r_0 \sin \tilde{\omega}t$$

The total radial velocity  $V_r$  can be composed from the two orthogonal components  $\hat{\theta}r$  and  $\dot{r}$ . One can easily find, again in the approximation  $K \ll 1$  that it corresponds to an helical motion with speed given by

$$\begin{aligned} V_r &\approx \frac{\dot{r}}{\sqrt{2} \pi \epsilon \eta^{1/2} B V^{1/2} r_0} \\ &= 6.06 \times 10^4 \frac{I}{B V^{1/2} r_0} \end{aligned}$$

The parameter which is relevant to our application is the ratio between the longitudinal and transverse speeds:

$$\Gamma = \frac{v_r}{\dot{z}} = \frac{I}{2\pi\epsilon\eta B V r_0} = 0.102 \frac{I}{B V r_0}$$

where  $\dot{z} = \sqrt{2\eta V}$ . Thus, as the magnetic field is made stronger and stronger, more and more electrons tend to travel in nearly straight lines from the cathode parallel to the beam axis and along the field lines. This method is more effective than the Brillouin solution. For the numerical case  $r = 1$  cm,  $\frac{I}{\pi r^2} = 10^4$  A/m<sup>2</sup>,  $V = 5 \times 10^4$  volt, we get now  $\Gamma = 6.41 \times 10^{-3}$  rad, which is considerably smaller than the Brillouin case. Note also that Budker et al.<sup>2</sup> have chosen  $I = 1$  A,  $r = 0.5$  cm  $B = 0.1$  Tesla and  $V = 5 \times 10^4$  volt giving with our formula at the beam periphery  $\Gamma = 4 \times 10^{-3}$  rad to be compared with the measured rms value  $\sim 3 \times 10^{-3}$  rad.

##### 5. General case of confined flow.

A more sophisticated form of confined flow is that in which the electron paths of the given region are designed to be along the lines of the field, which is no longer constant. The treatment presented here is due to Kleen and Pöschl.<sup>7</sup> The set-up is the one shown in Fig.13. The magnetic shield is adjusted until the electron trajectories near the cathode surface lie along the magnetic field lines. The Equation (6) can be rewritten after some manipulations in the form:

$$\frac{B_0^2}{B_z^2} \frac{r_0^4}{r_m^4} + \frac{2\sigma}{r_m^2} \pm 1 = 0$$

where 
$$\sigma = Kr_0^2 = \frac{3.5 \times 10^{-7} I_0}{B_z^2 V^{1/2}}$$

Then:

$$r_m = \sigma^{1/2} \left( 1 + \sqrt{1 + \frac{B_0^2 r_0^4}{B_z^2 \sigma^2}} \right)^{1/2}$$

As before we put  $r = r_m(1 + \delta)$ , and use expansion approximations to obtain:

$$\frac{d^2\delta}{dt^2} + 2(A + 1)\omega_L^2\delta = 0$$

where

$$A = \left( \frac{B_0 r_0^2}{B_z r_m^2} \right)^2, \quad 0 \leq A \leq 1$$

Then  $\delta = C_1 \cos \sqrt{2(A+1)} \omega_L t + C_2 \sin \sqrt{2(1+A)} \omega_L t$ .

The origin is taken at the aperture separating region 1 from region 2 (see Fig. 14). Let  $r = r_a$  at the origin and let the beam be converging to the axis by an angle  $\alpha_0$ . Then,

$$C_1 = \frac{r_a - r_m}{r_m} \quad C_2 = \frac{u_0 \tan \alpha_0}{\sqrt{2(1+A)} \omega_L r_m}$$

The maximum radius is then given by:

$$\frac{r_{\max}}{r_{\min}} = 1 + \frac{r_a}{r_m} \sqrt{\left( \frac{r_m}{r_a} - 1 \right)^2 + \frac{1}{2(A+1)} \left( \frac{u_0 \tan \alpha_0}{\omega_L r_m} \right)^2}$$

The value of  $\frac{r_{\max}}{r_{\min}} \rightarrow 1$  only if  $\frac{r_m}{r_a} \rightarrow 1$  and also the second term

under the radical goes to zero, i.e.  $\alpha_0 \rightarrow 0$ . If this is achieved then the beam at high field will be smooth and uniform.

Finally, in order to compare various experimental situations, we shall derive a useful relation between the magnetic flux enclosed by the mean diameter  $2r_m$  and the flux through the cathode surface, at optimum adjustment settings. We define the flux ratio  $\alpha$  as

$$\pi r_o^2 B_o = \alpha \pi r_m^2 B_z$$

i.e.

$$\alpha = \frac{r_o^2 B_o}{r_m^2 B_z} = A^{1/2}$$

Then for  $\ddot{r} = 0$ , i.e.,  $r = r_m$ , we can rewrite Eq.(6) as follows:

$$\frac{\omega_p^2}{2P} = \omega_L^2 (1 - \alpha^2)$$

or alternatively

$$\alpha^2 = 1 - \frac{\omega_p^2}{2\omega_L^2}$$

In the Brillouin case  $\omega_p^2 = 2\omega_L^2$ , therefore  $\alpha^2 = 0$  and no flux hits the cathode. In the uniform field case  $\omega_p^2/z\omega_L \rightarrow 0$  and  $\alpha^2 \rightarrow 1$  and all the flux goes through the cathode. For instance, at twice the Brillouin field  $\alpha \sim 0.86$ . The percentage of flux cutting the cathode grows very rapidly once  $2\omega_L^2 > \omega_p^2$ . Using the Bush theorem we get

$$\dot{\theta} = \omega_L (1 - \alpha).$$

Which shows that the minimum angular divergence of the beam can be achieved with  $\alpha \approx 1$ , i.e., the flux must thread the cathode for maximum cooling efficiency.

5. Discussion.

There are several questions which deserve further consideration:

- (a) Is flow stable? The answer to this question is in general , yes. We refer to the book of Pierce for details.
- (b) All the theory is based on laminar flow, i.e., the trajectories do not cross each other. This assumption is not completely correct.<sup>8</sup> Some experimental work is needed to clear up the implication of such a simplifying assumption.
- (c) Effects of thermal velocities. Again the effect are expected to be small.
- (d) Matching around the accelerating region near the cathode and e.s. lens effects around the cathode. Some jump of radial velocity are expected and they must be investigated.
- (e) Positive ions effects. Positive ions can easily neutralize the space charge of the beam and modify the present discussion

It is expected however that the present treatment elucidates the most salient features of the device, and constitutes a valid guide to the construction of an experimental prototype.

References

1. G. I. Budker; Report on International Conference, Orsay 1966.
2. V.V. Anashin, et al. Set up for electron cooling experiments, Report IYaF74-86, USSR Academy of Sciences Siberian Division (in Russian).
3. Brillouin, Phys. Rev. 67, 260 (1945).
4. Samuel, Proc. IRE, 37, 1252 (1949).
5. Wang, Proc. IRE 38, 135 (1950).
6. J. R. Pierce, Theory and Design of Electron Beams, D. Van Nortrand Co., New York (1954).
7. Kleen and Pöschl; AEU 9, 295 (1955).
8. Harker, Jour. Apl. Phys. 28, 645 (1957).

Appendix III Freezer Ring as an Accumulator and Proton Cooler  
to Increase Luminosity

It appears that the Freezer ring might be useful to decrease the emittance of the booster proton beam in normal operation and possibly increase the luminosity for  $\bar{p}p$  colliding beams.

One problem with the Fermilab booster system presently comes from the horizontal aperture limitation which is  $\sim 30\pi$  rather than the theoretical  $90\pi$ . This aperture prohibits the originally planned radial 4-turn injection from the linac; the emittance from the linac is  $\sim 10-15\pi$  for currents of 250 mA. Furthermore, the linac is running idle most of the time, being used only  $\sim 3\mu\text{sec}$  for every booster cycle (66 msec). Increasing the linac current increases the emittance and does not lead to large gains in the current stored in the booster.

There is one obvious and simple solution - decrease the emittance of the linac beam and store the linac beam during the "idle" times. The Freezer ring is potentially extremely useful for this purpose provided electron cooling of the beam takes place in times comparable to the booster repetition rate.

The basic scheme would be to inject the linac beam into the Freezer ring during the idle time of  $\sim 66$  msec. Multi-turn injection could be accomplished if the electron cooling time can be decreased to  $\sim 20-30$  msec. The cooled proton beam is then injected into the booster after the normal injection cycle. The current in this reduced emittance beam will be limited by space charge in the booster. Several kinds of

problems related to tune shift, resistive wall instability, non-linear resonances, etc., depend strongly on emittance, and should become much more controllable than at present. Additionally, synchronous transfer from the Freezer to the Booster should improve the rf capture efficiency. This would result ultimately in improved luminosity.

Table I. Parameters of  $\bar{p}$  injection  
and deceleration in the Booster.

Antiproton injection energy (kinetic)	$T_{\bar{p}}$	5.717 GeV
Target length and material	$l_t$	5cm, tungsten
Target efficiency		0.3
Proton beam size at target		$\cong 0.5$ mm
Betatron function of $\bar{p}$ 's at target center		
- vertical betatron	$\beta_V^*$	0.025 m
- horizontal betatron	$\beta_H^*$	0.025 m
- momentum dispersion	$\chi_p^*$	$\approx 0$
Acceptances of the Booster ring at 200 MeV		
- vertical	$A_V$	$40\pi 10^{-6}$ r.m.
- horizontal	$A_H$	$40\pi 10^{-6}$ r.m.
- longitudinal	$A_0$	3 eV sec
Acceptances from the target		
- production angle	$\theta_{pwi}$	$0^\circ$
- solid angle	$\Delta\Omega$	$5.3 \times 10^{-4}$ sterad
- momentum acceptance ( $B = -.12$ )	$\Delta p$	2.0 MeV/c
Antiproton yield for incident proton	$\bar{p}/p$	$0.83 \times 10^{-6}$

Table II. Major Beam Transfer Elements

<u>Element</u>	<u>Description</u>	<u>Length</u>	<u>Field</u>	<u>Deflection Angle</u>
S1	Fast Magnetic Kicker	7m	0.05 T	1.0 mrad
S2	Lambertson Septum(2)	7m	0.9T	20 mrad
B1	Fast Magnetic Kicker(2)	2.5m	0.06T	7 mrad
B2	Pulsed Current Sheet Septum	5m	0.3T	70 mrad

<u>Quadrupole</u>	<u>Length (m)</u>	<u>Half Aperture (cm)</u>	<u>Gradient (Tm<sup>-1</sup>)</u>
Q1	1.0	7.0	+1.560
Q2	1.0	9.0	-1.365
Q3	1.0	3.0	-1.950
Q4	1.0	2.0	-2.925
Q5	1.0	2.0	+0.780
Q6	1.0	2.0	-0.975

Table III Tentative parameters of the Freezer Ring

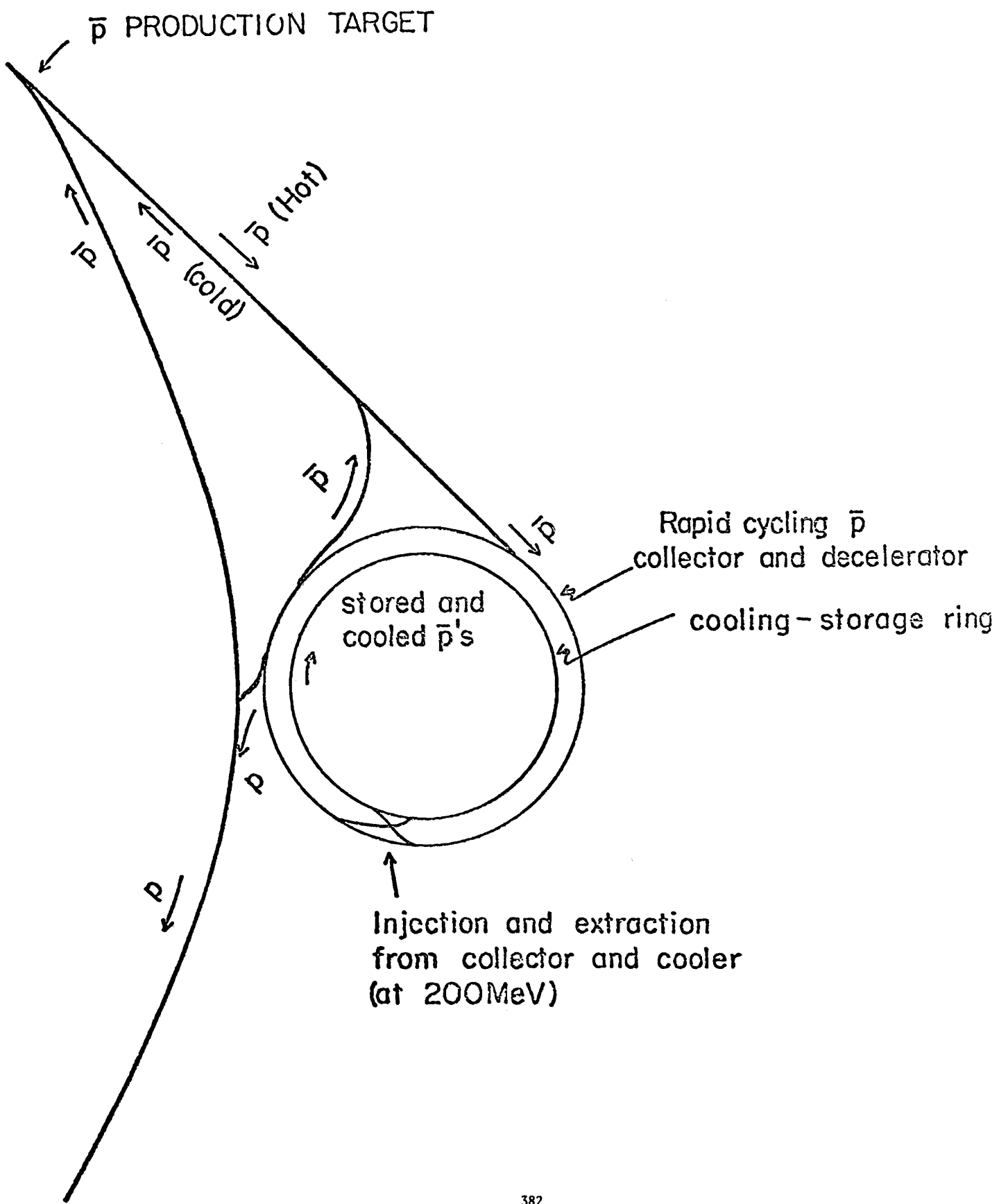
Nominal momentum	$p_0$	644 MeV/c
Guide field	$B_0$	0.5T
Magnetic radius	$\rho$	4.3 m
Orbit radius	R	75 m
Focussing Type	separated function	
Number of cells		12
Length of each cell		39.3 m
Rotation functions:		
- maximum value	$\beta_{max}$	27 m
- of the cooling sections	$\beta_{straight}$	15 m
Momentum compaction	$x_p \text{ max}$	6 m
Transition - energy	$x_p \text{ straight}$	$\sim 2 \text{ m}$
	$\gamma_t = 9$	
Length of cooling straight sections		7.5 m
Betatron acceptance	$E_H$	$96\pi \cdot 10^{-6} \text{ m}$
	$E_V$	$75\pi \cdot 10^{-6} \text{ m}$
Momentum acceptance	$\Delta p/p$	$\pm 5 \cdot 10^{-3}$
Phase advance per cell	$\phi_x$	0.27
	$\phi_y$	0.26

Table IVa. Freezer Ring Dipole

Field Strength	0.5T
Magnet Length	1.0m
Magnet Gap	3"
Pole Aperture	12"
Field Aperture	6"
Field Quality	±0.1%
Coil Turns(Top + Bottom)	140
Copper Conductor Cross Section	.325" x .325"
Water Cooling Hole Diameter	.181"
Conductor Corner Radius	.063"
Conductor Current	220 A
Magnet Inductance	.006 H
Coil Resistance	.12 Ω
Voltage Drop	26 V
Power	5.7 kW
Cooling Water Pressure	150 psi
Number of Water Paths	4
Water Flow	1.4 GPM
Temperature Rise	20°C
Outside Dimensions	25" x 15"
Iron Weight	3000 Lb.
Copper Weight	300lb.

Table IVb. Freezer Ring Quadrupole

Field Gradient	10 T/m
Magnet Length	10"
Aperture	8" dia.
Width of Good Field Gradient	±5"
Gradient Quality ( $\Delta B/B$ at 1.5" Rad.)	±.1%
Coil Turns per Pole	30
Copper Conductor Cross Section	.325" x .650"
Water Cooling Hole Diameter	.128"
Conductor Corner Radius	.981"
Conductor Current	300A
Magnet Inductance	.010H
Coil Resistance	.011 $\Omega$
Voltage Drop	3.3 V
Power	1.0kW
Cooling Water Pressure	150 psi
Number of Water Paths	1
Water Flow	0.6 GPM
Temperature Rise	8 °C
Outside Dimensions	27" dia.
Iron Weight	1300 lb.
Copper Weight	200 lb.



382  
**FIG - 1**

# MAIN RING CYCLE DURING $\bar{P}$ PRODUCTION

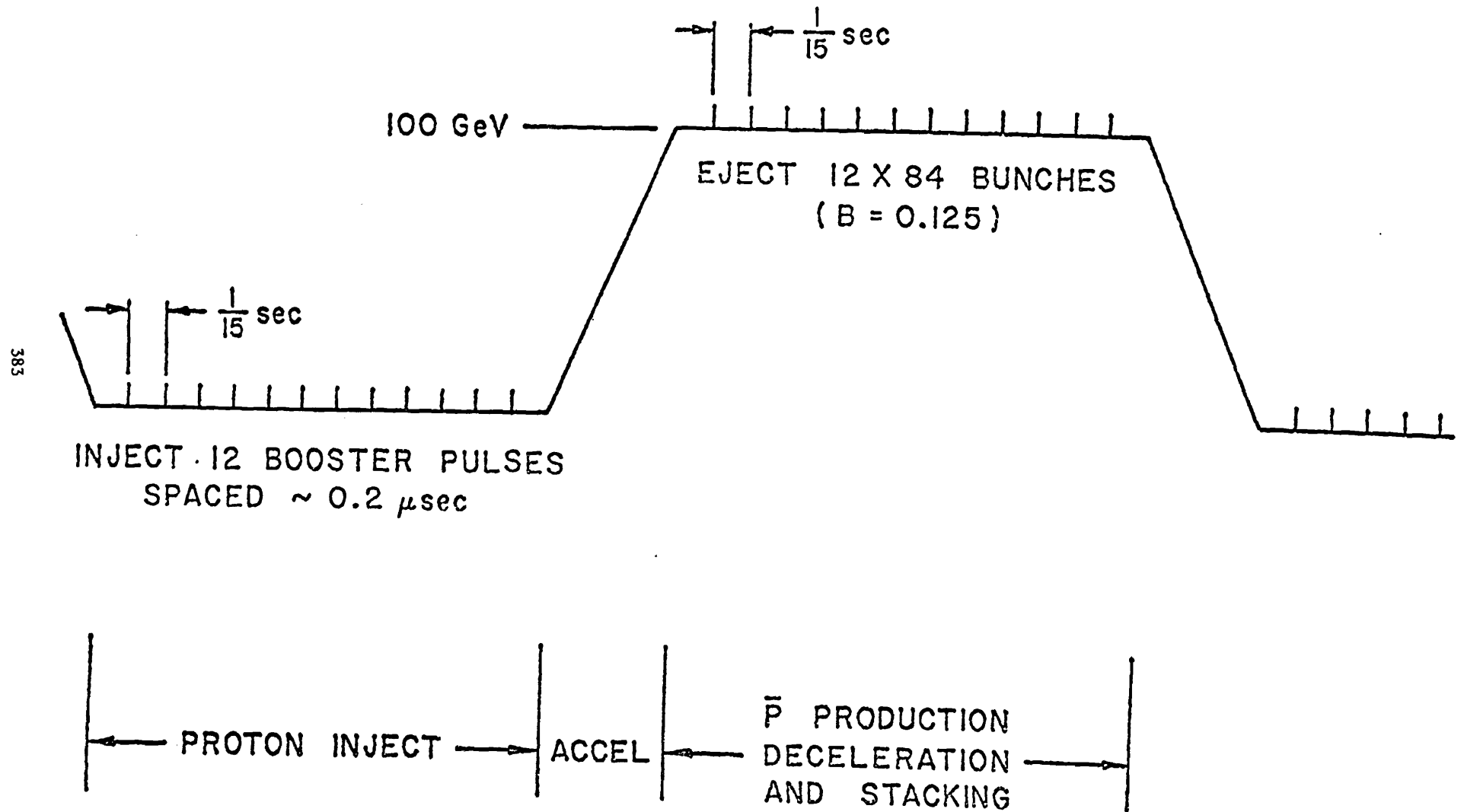


FIG - 2

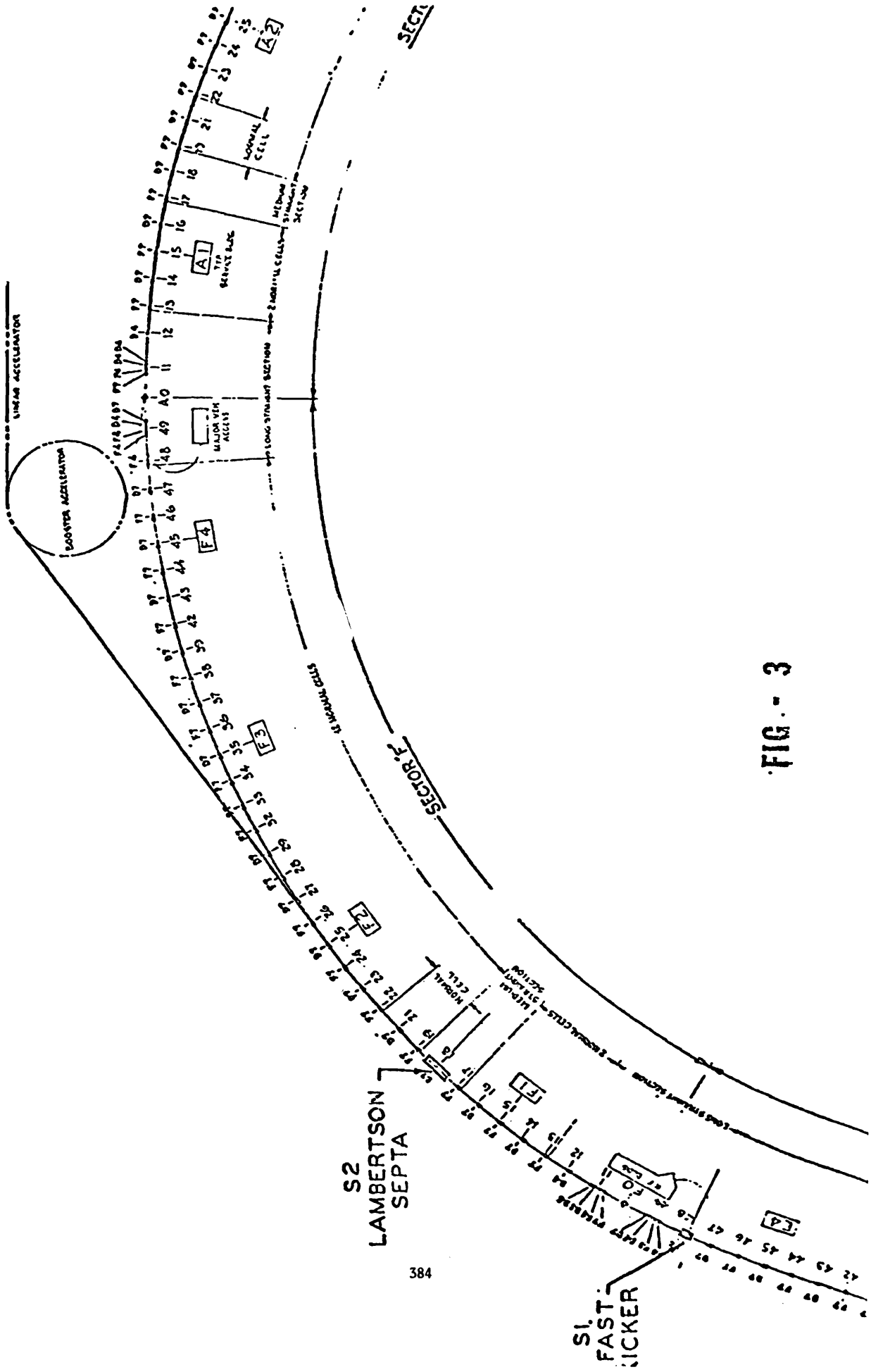


FIG. - 3

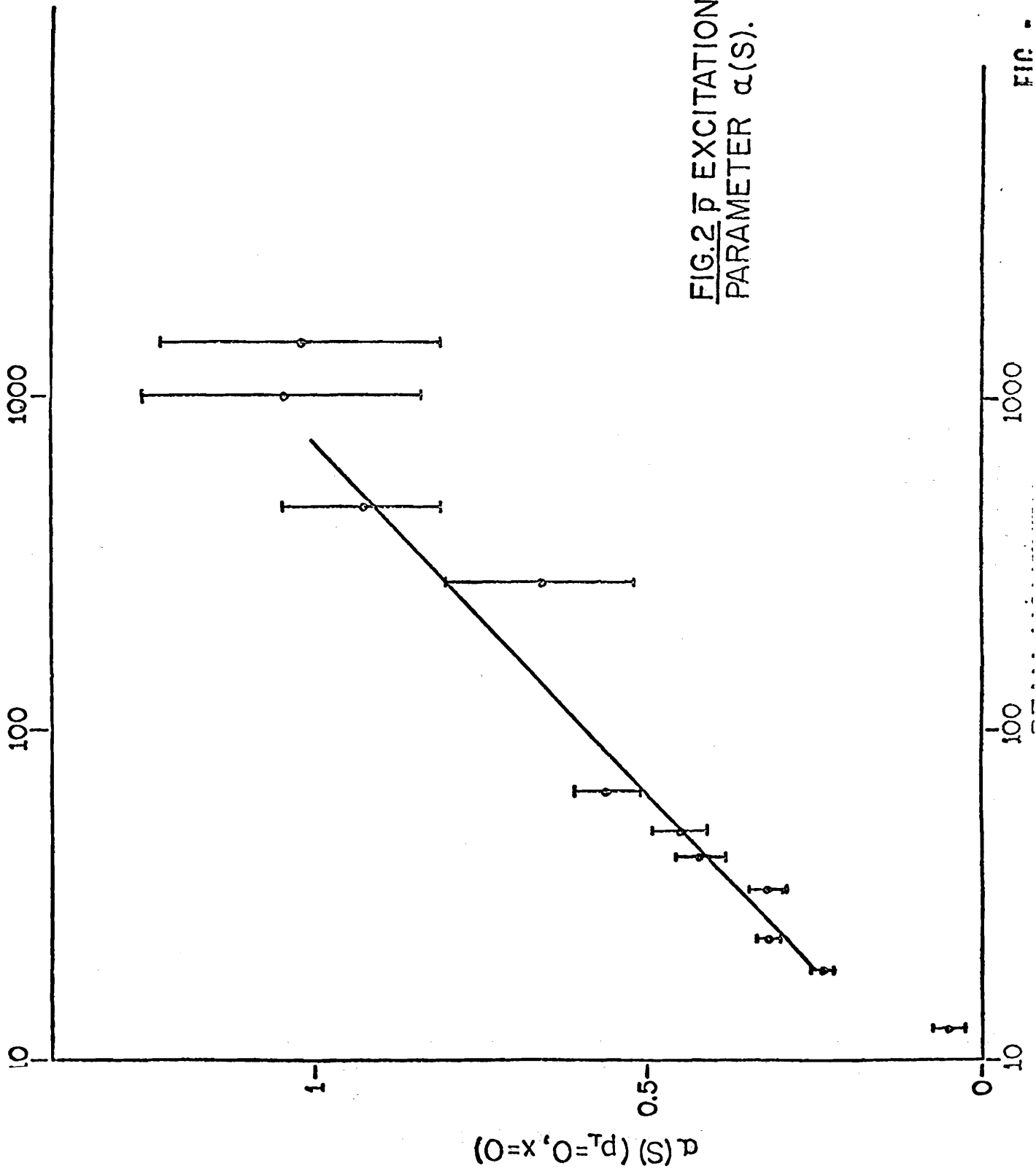


FIG. 2  $\bar{p}$  EXCITATION  
PARAMETER  $\alpha(S)$ .

FIG - 4

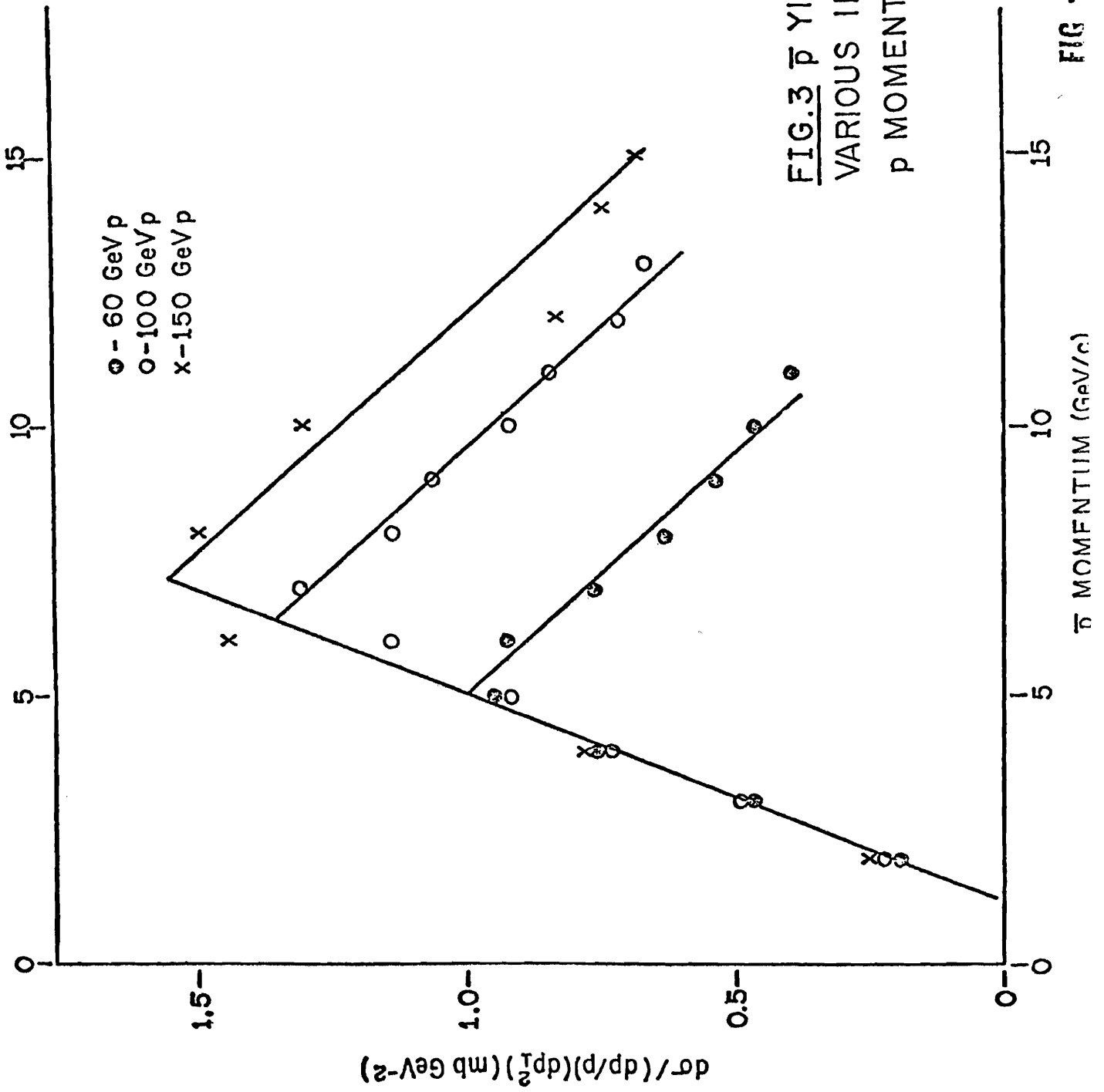


FIG. 3  $\bar{p}$  YIELD FOR  
 VARIOUS INCIDENT  
 p MOMENTA.

FIG - 5

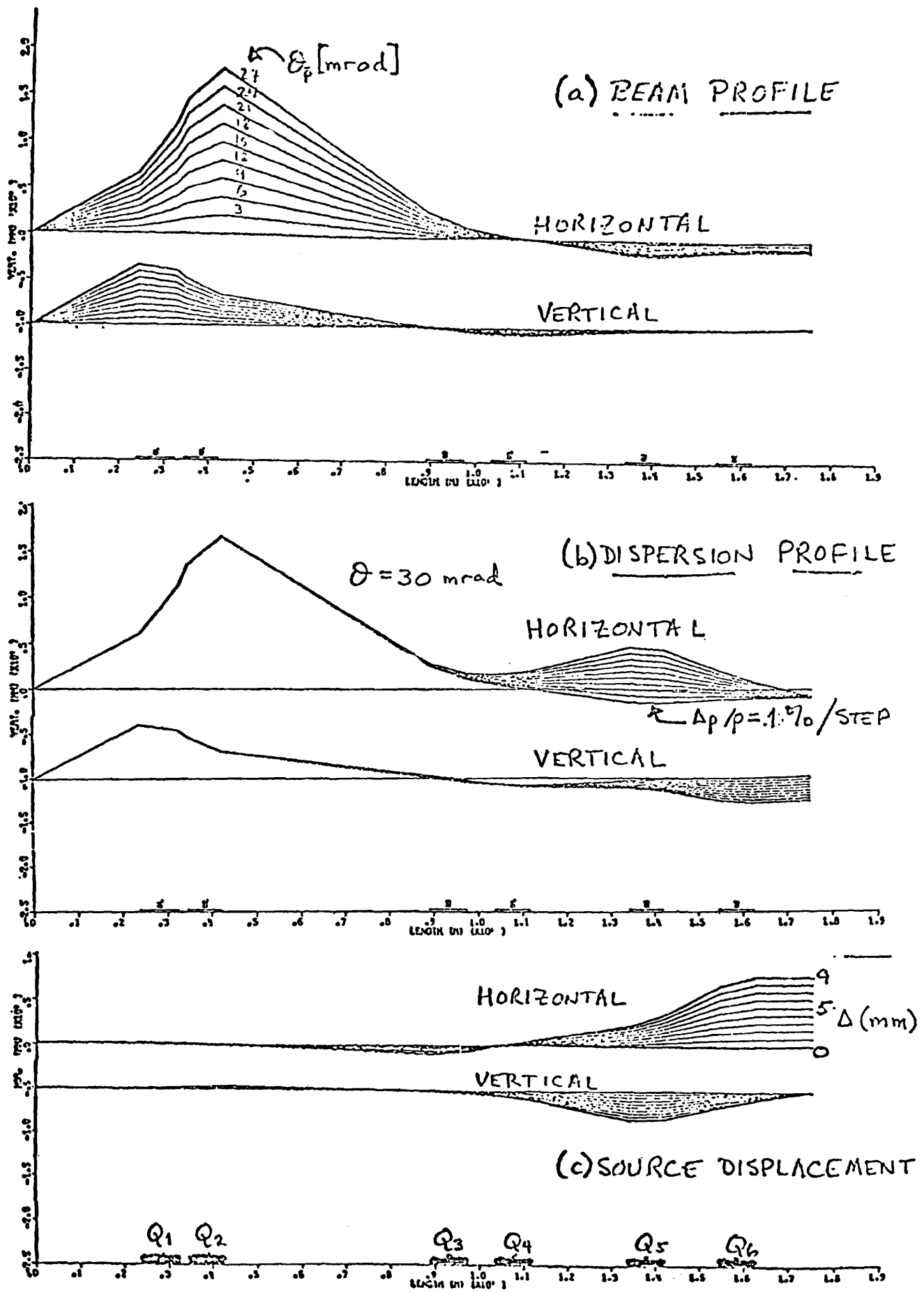
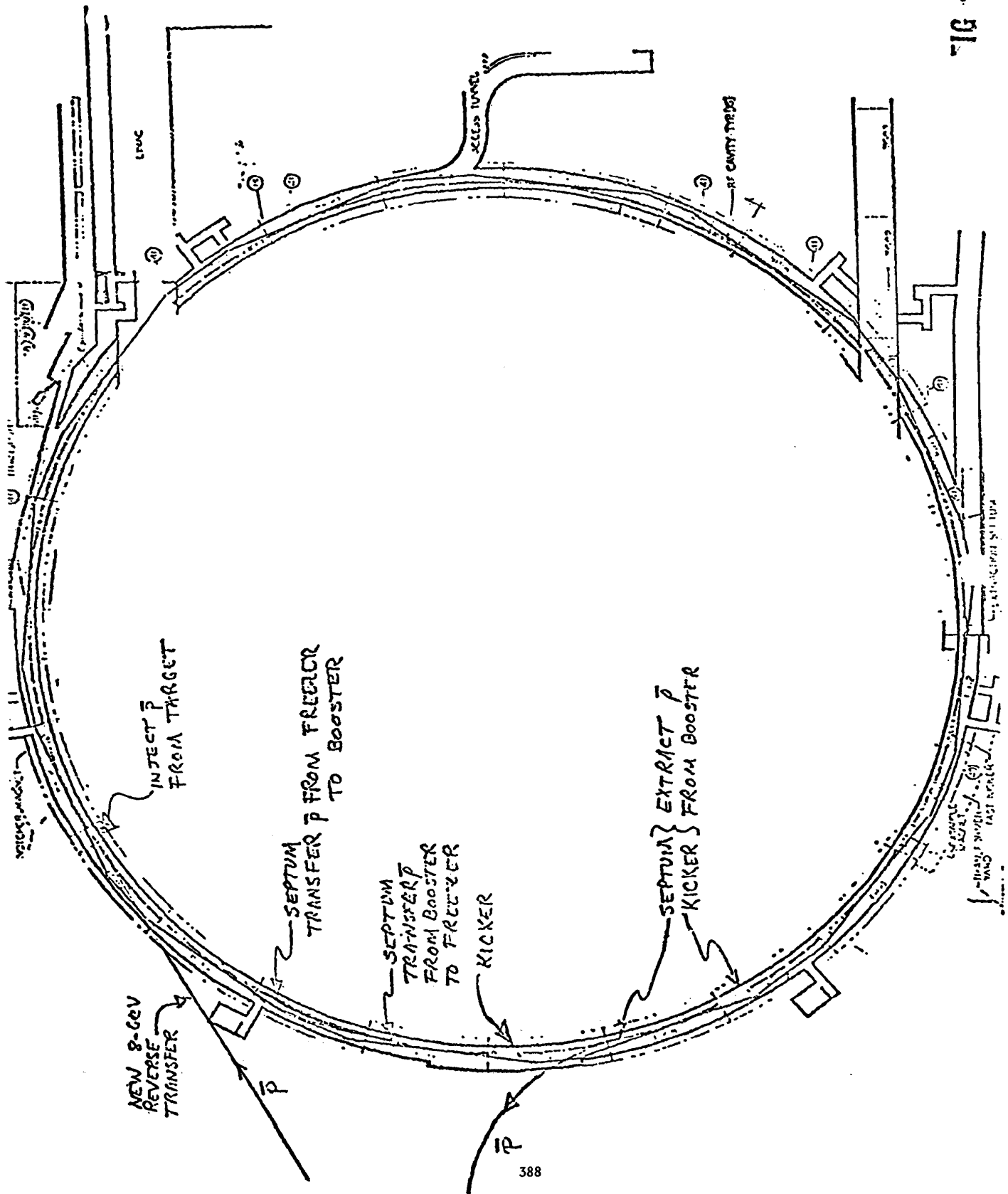
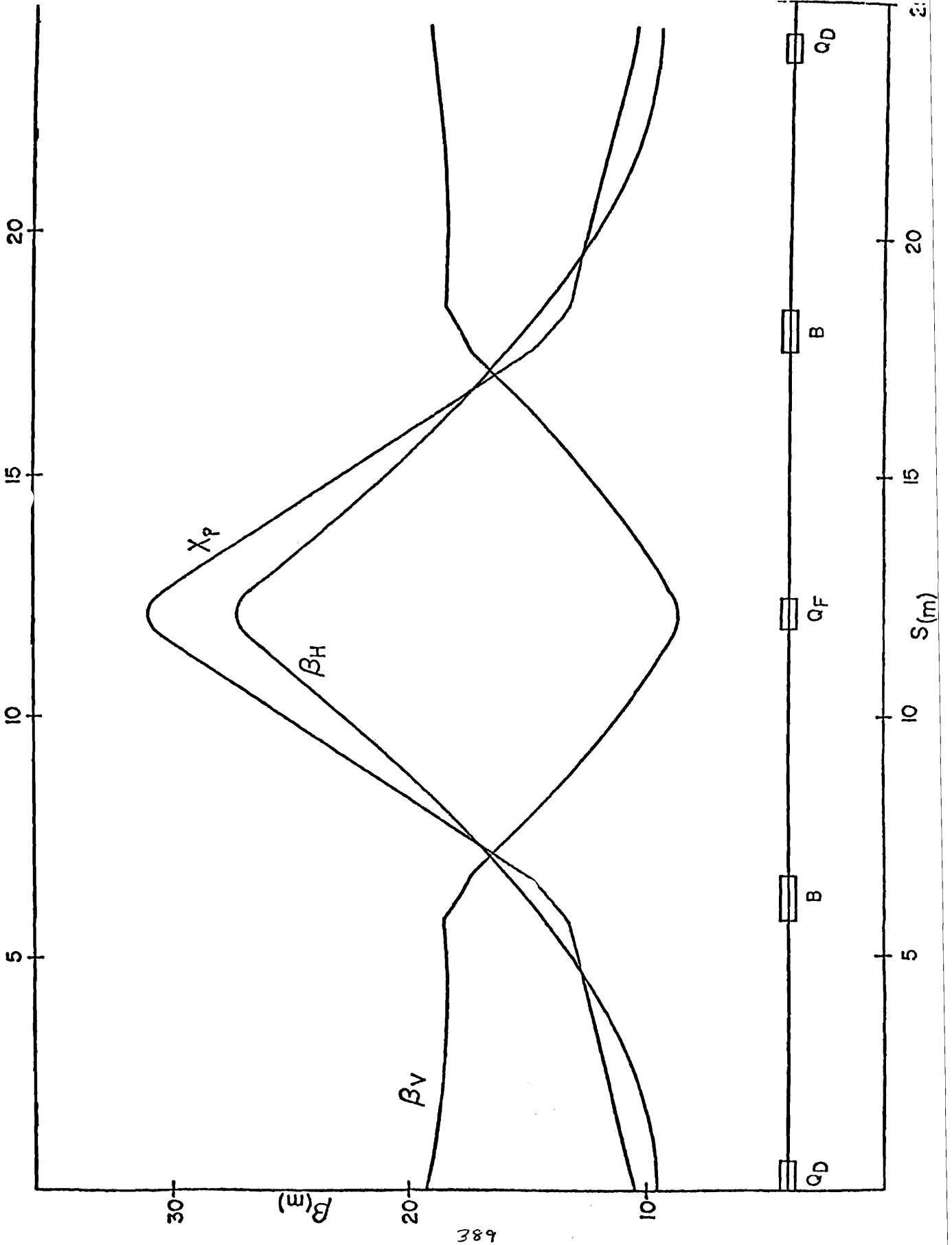


FIG - 6 387





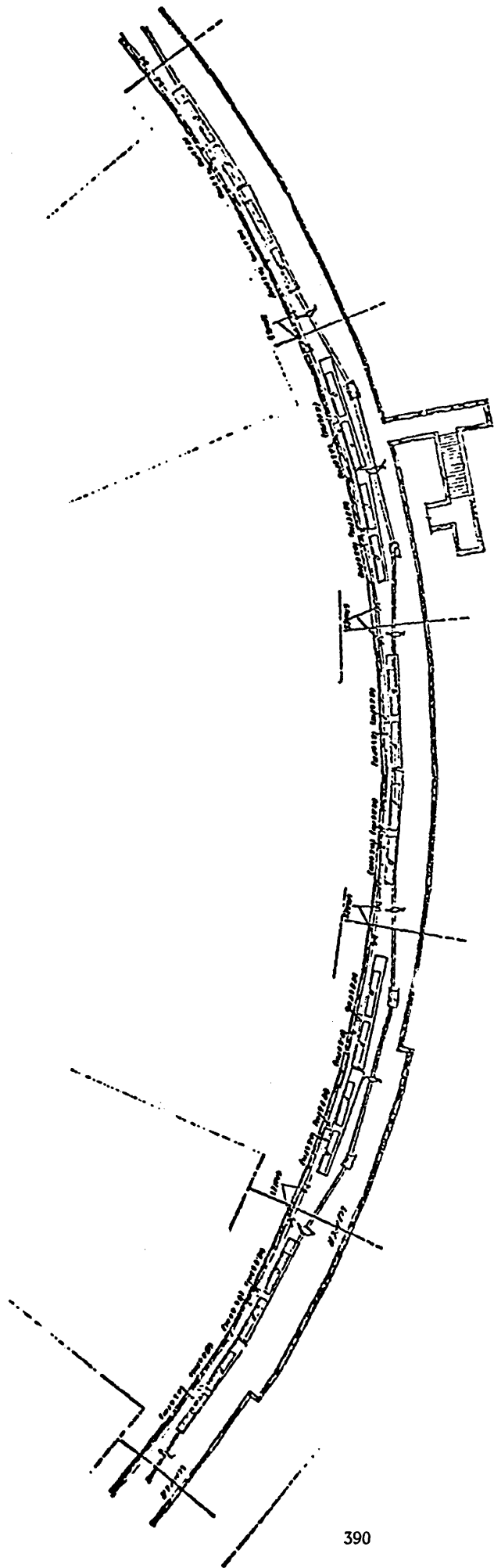


FIG - 9

BSR BEAM PIPE  
AT MIDDLE OF BOOSTER BEND  
(MINIMUM RADIUS)

BSR BEAM PIPE  
AT MIDDLE OF BOOSTER STRAIGHT

BSR DIPOLE  
(MAXIMUM RADIUS)

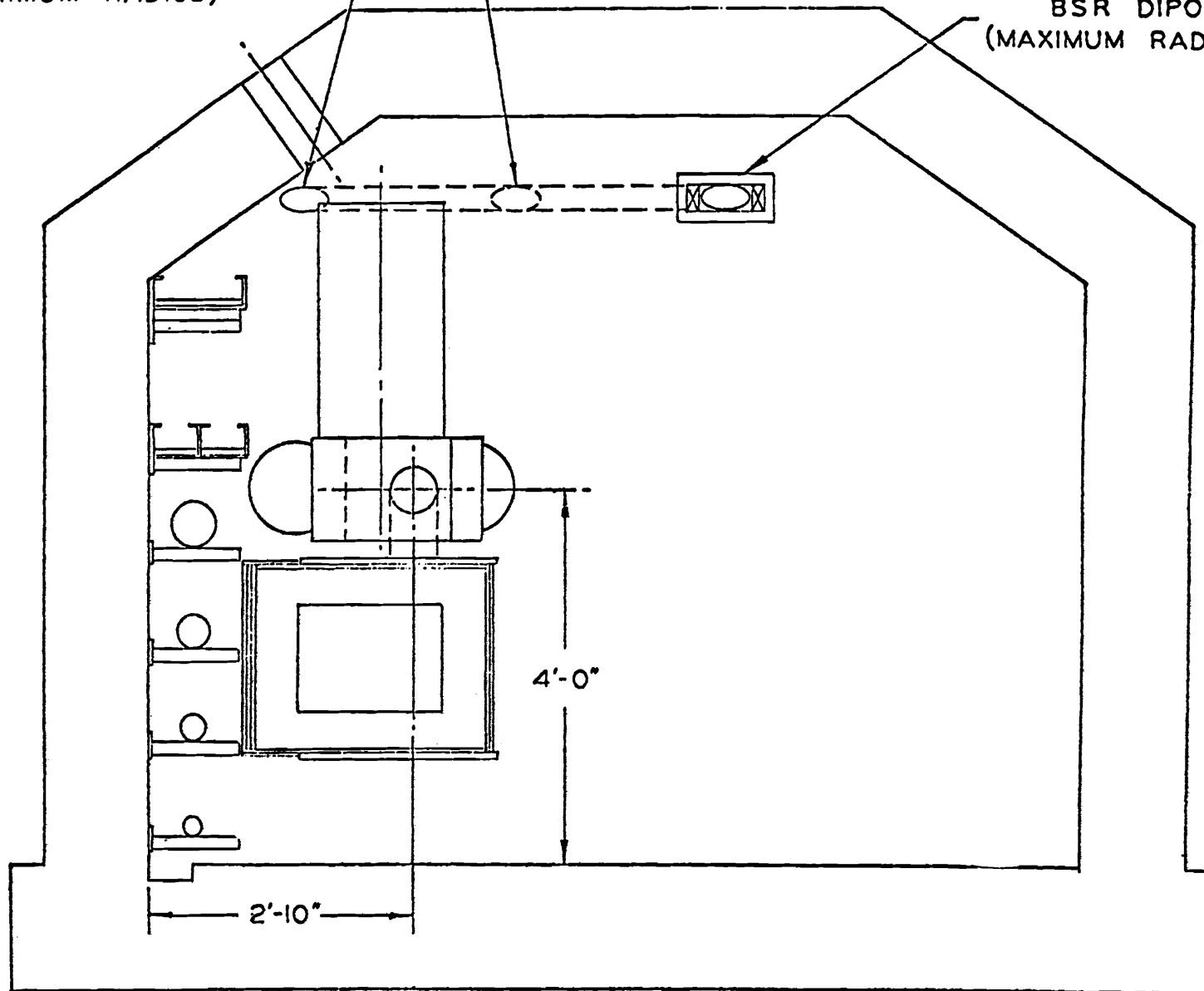
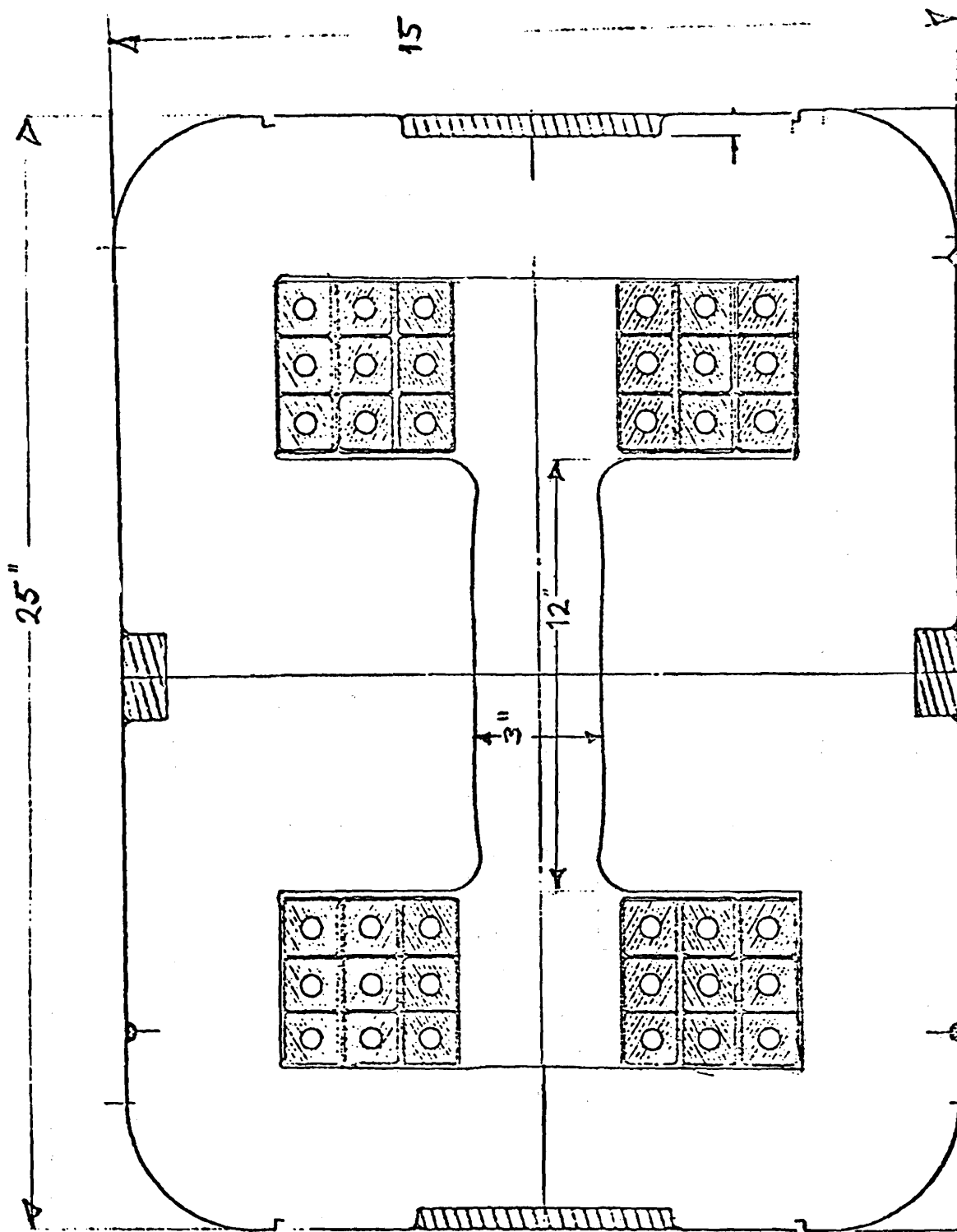


FIG - 10



FIG

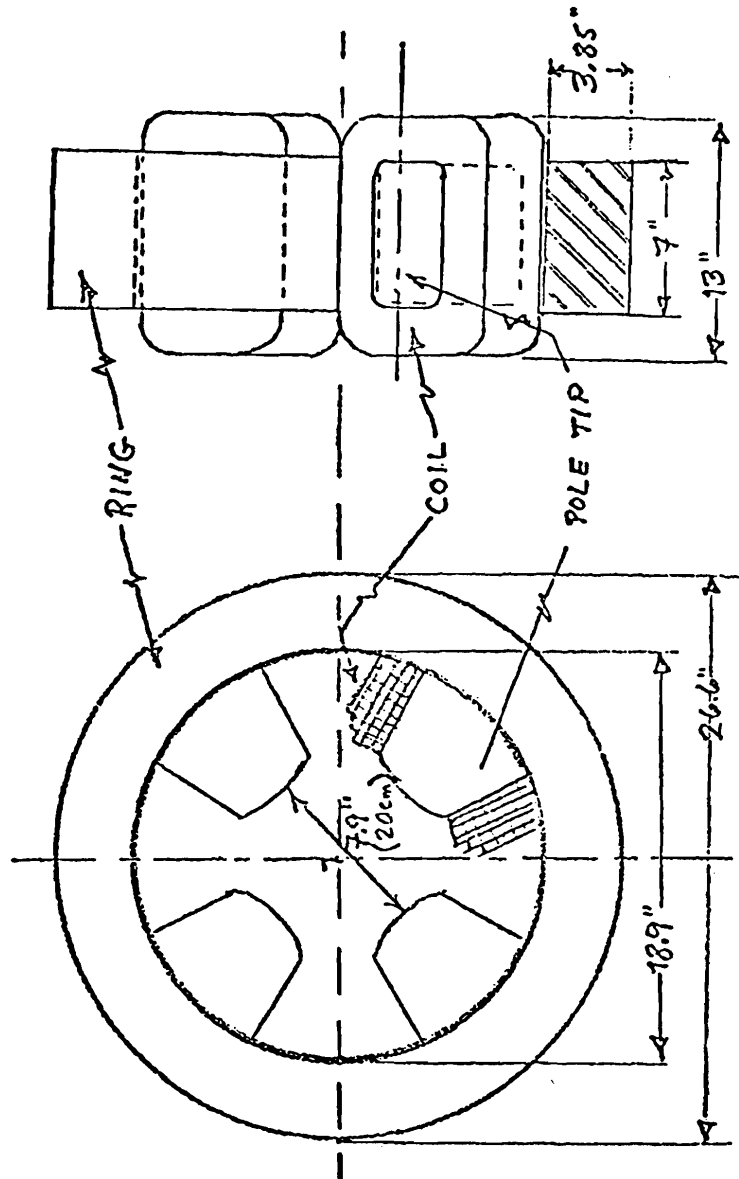
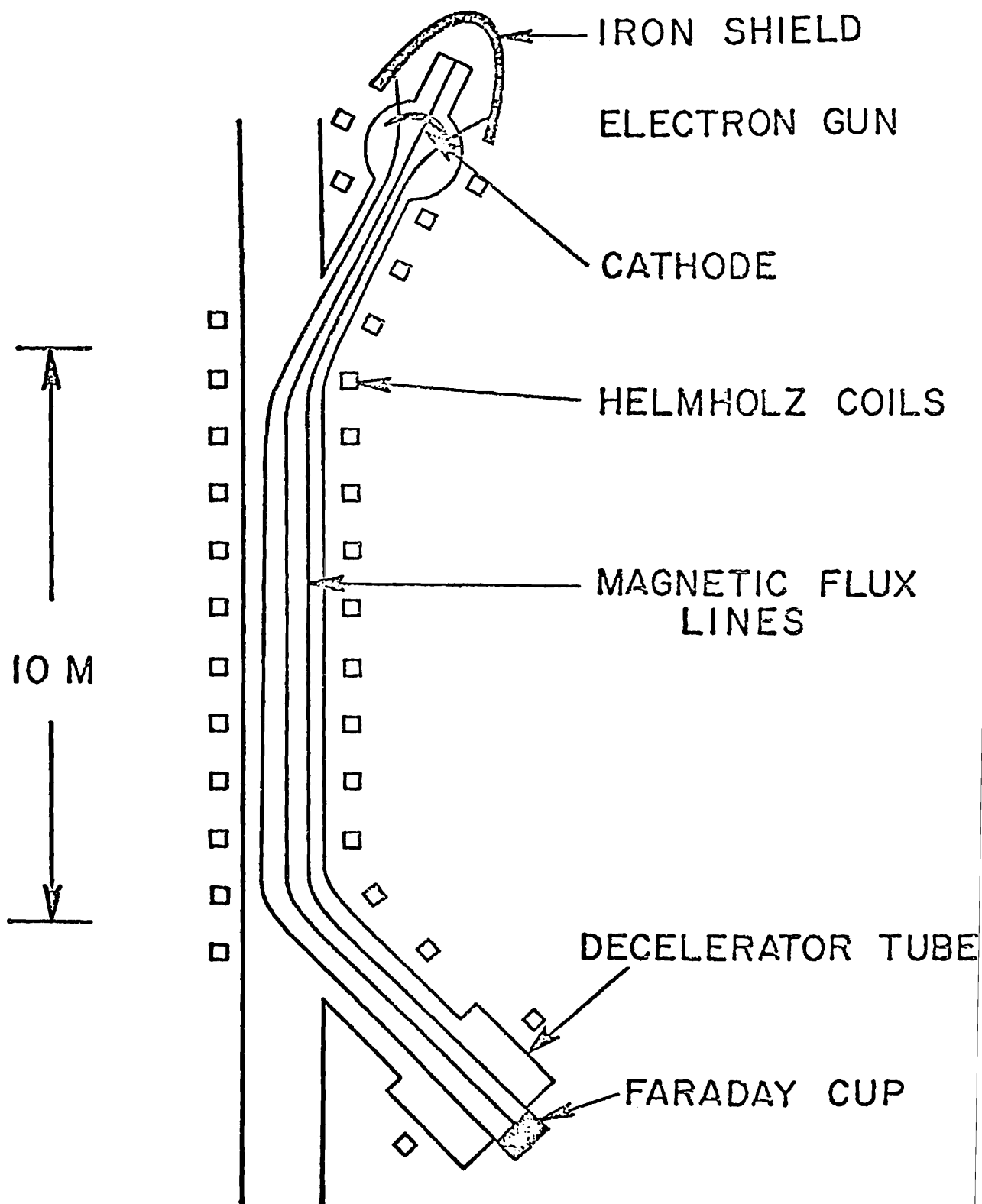


FIG - 12

# Cooling Straight Section (Schematic)



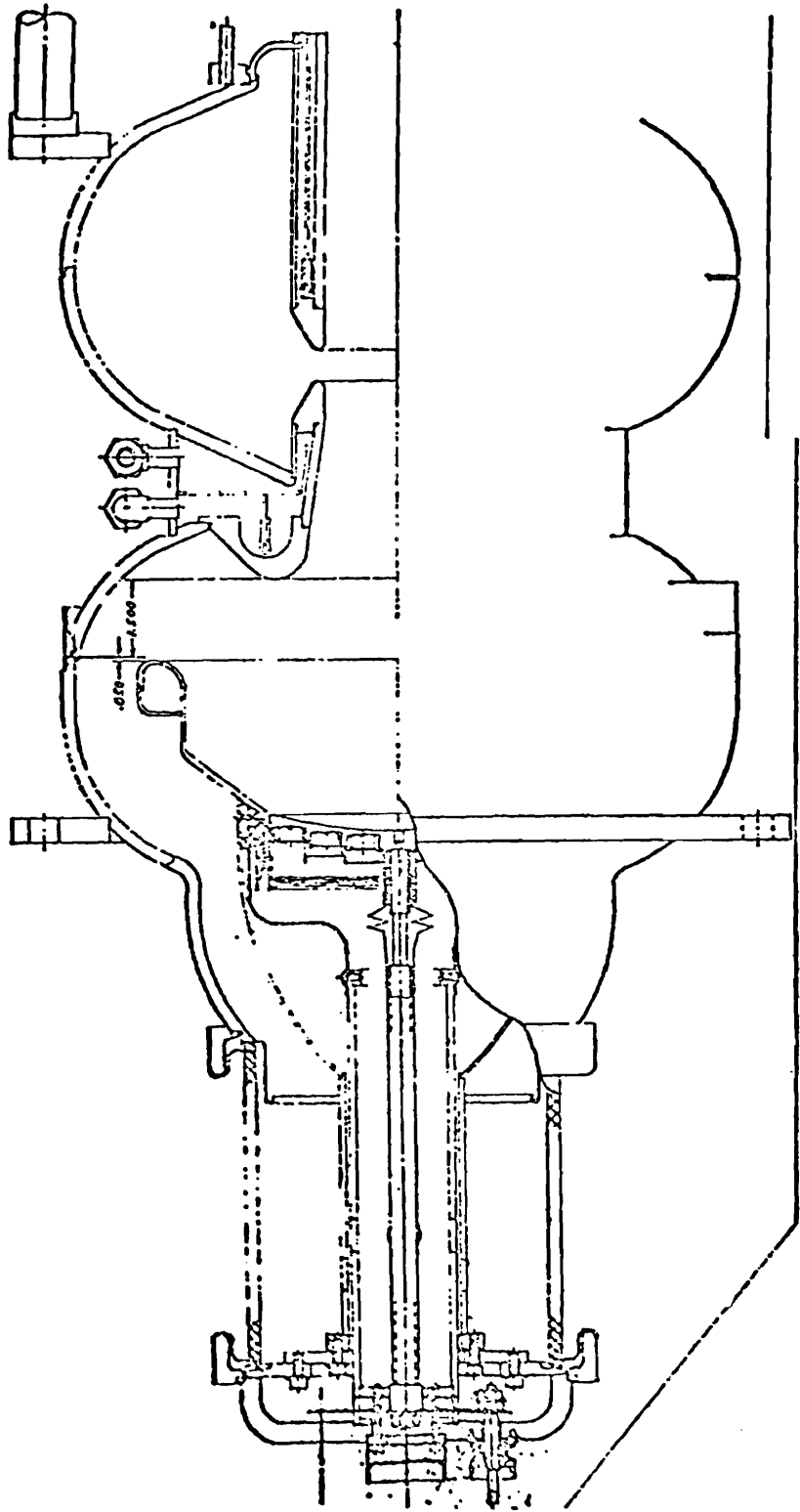


FIG - 14

Schematic of Stacks in the Freezer

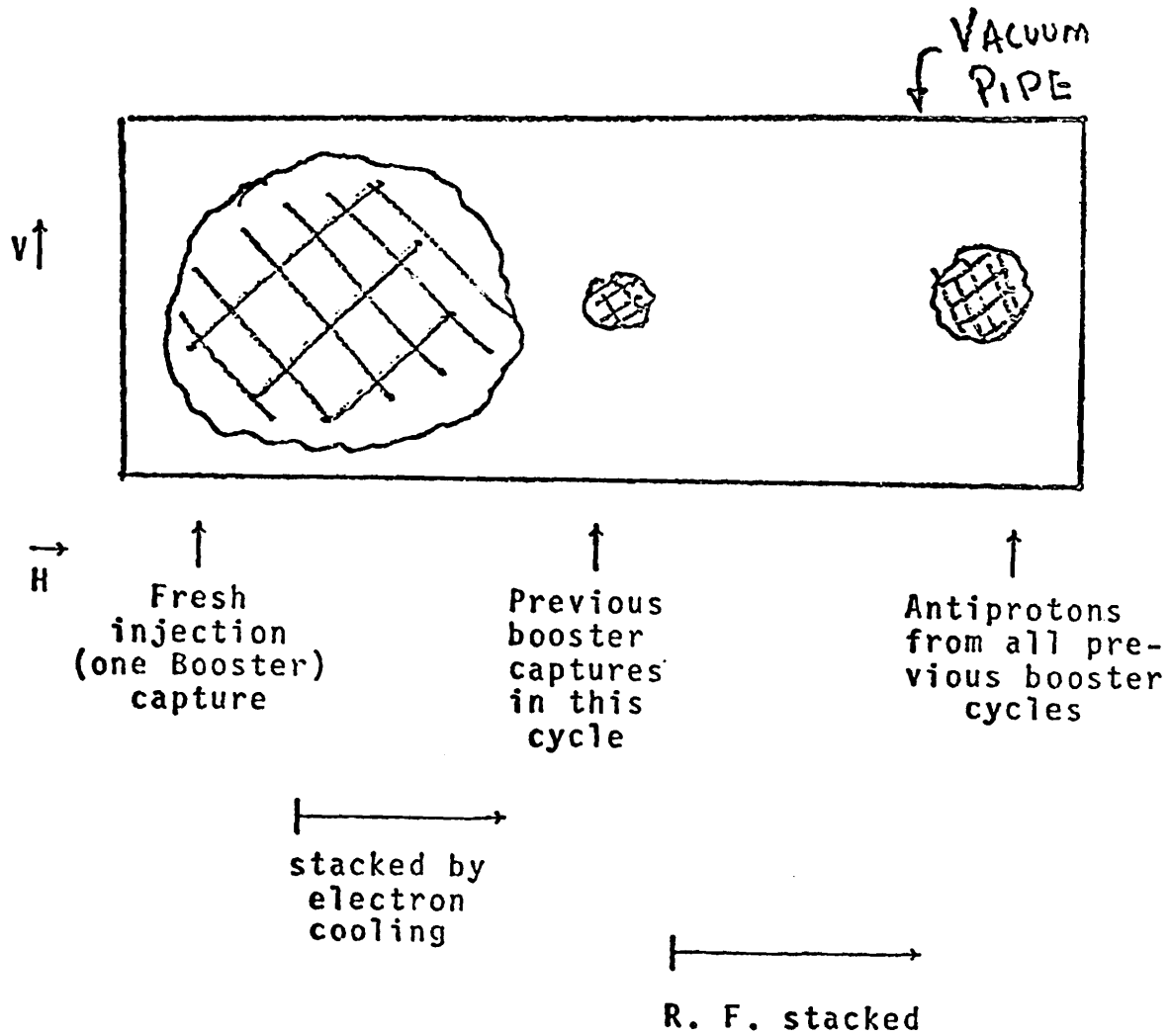
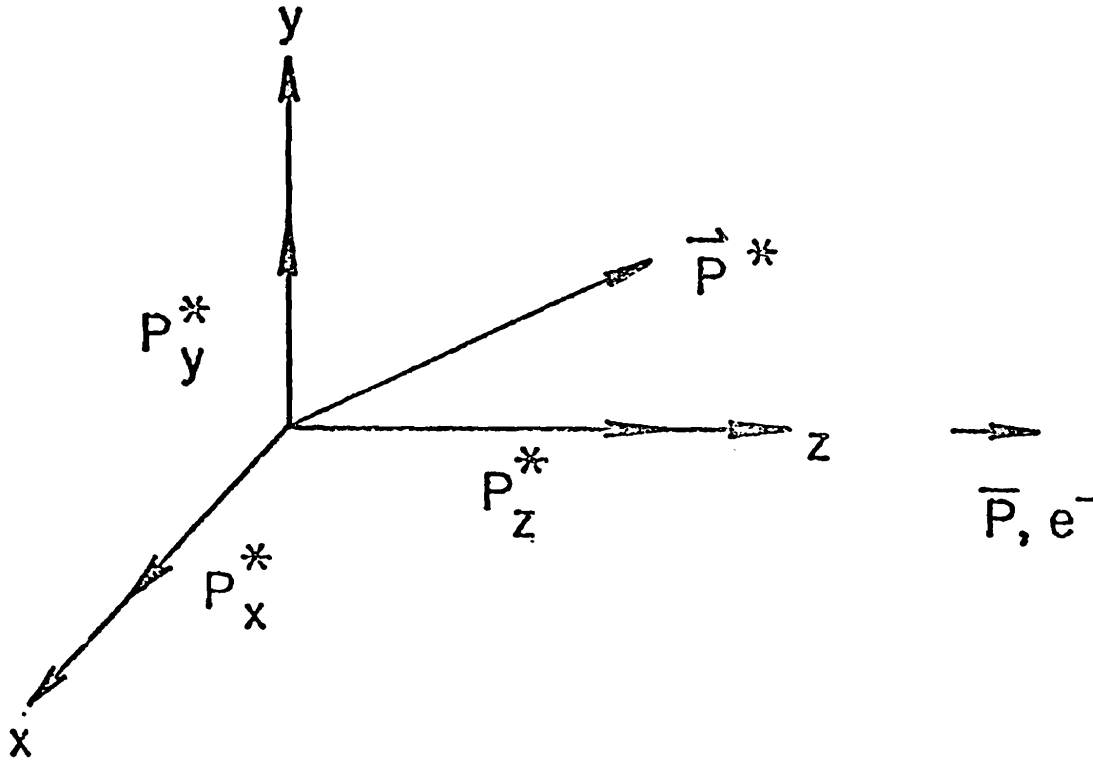


FIG - 15

# Motion of Antiprotons in the Electron Rest System



$$P_x^* \text{ and } P_y^* \propto f(t)$$

$$P_z^* \sim \text{const.}$$

FIG - 16

# UNIT CELL (DOFOD)

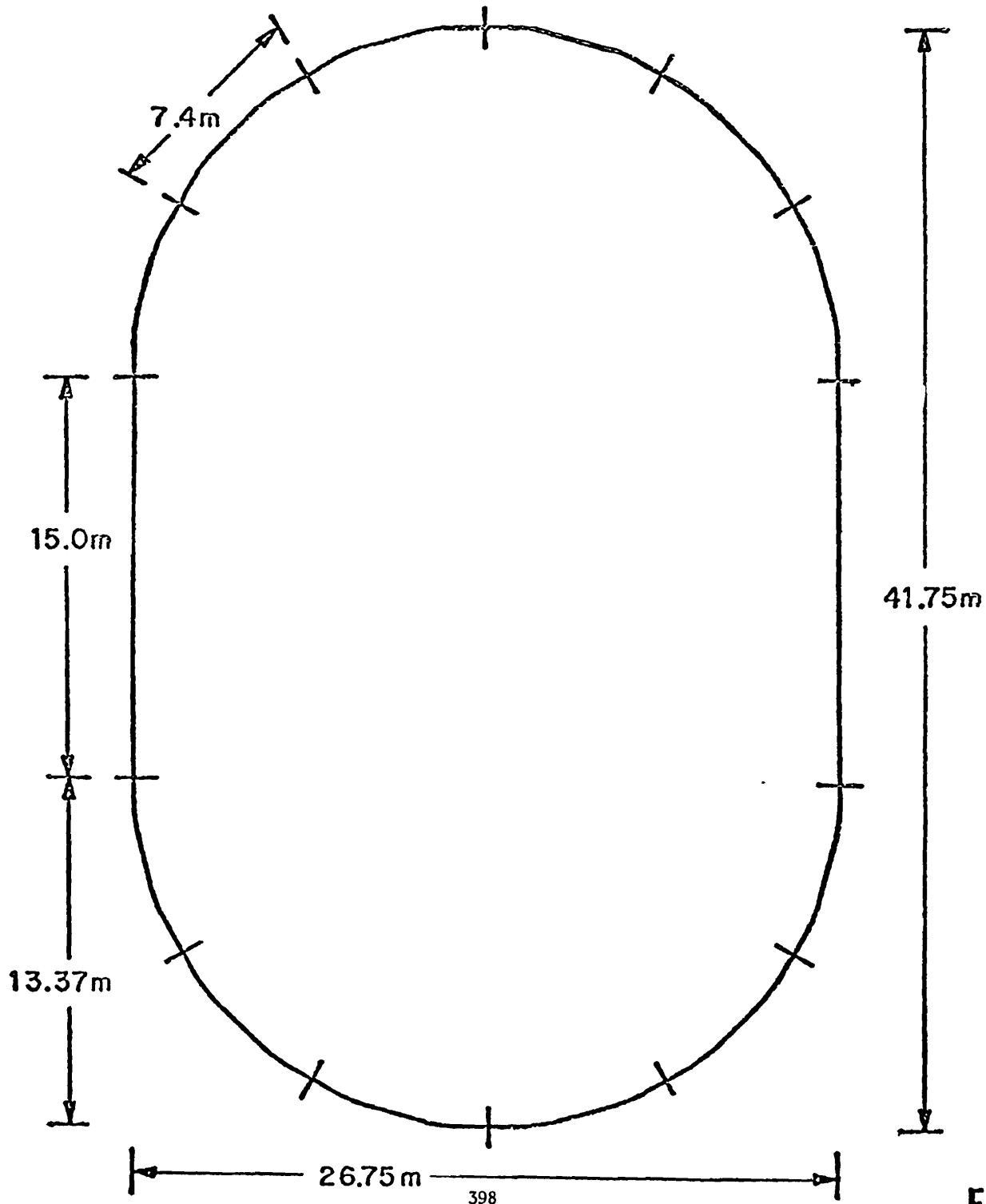
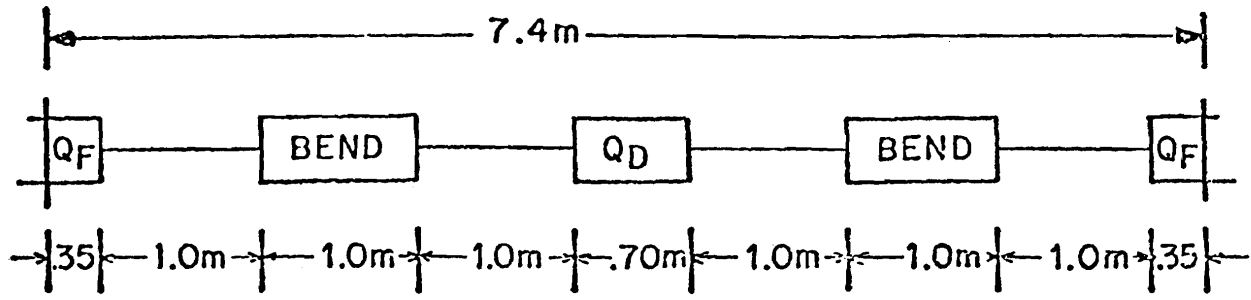


FIG - 17